

1 Journal: Ecosphere

2 Manuscript Type: Article

3

4 **Trading off nature for nature-based solutions: the bioeconomics of forest**

5 **management for wildlife, timber and carbon**

6

7 Jonah Ury, Matthew J. Kotchen, and Oswald J. Schmitz\*

8

9 School of the Environment, Yale University 195 Prospect Street, New Haven, CT 06511 USA

10

11 \* Author for correspondence: [oswald.schmitz@yale.edu](mailto:oswald.schmitz@yale.edu)

12

13

14

15 Open Research Statement: The code to conduct numerical analyses is provided at

16 <https://doi.org/10.5061/dryad.j0zpc86p1>

17

18 **KEYWORDS:** ecosystem dynamics; financing carbon capture, bioeconomic modelling, wildlife  
19 control over ecosystem functioning.

20

21

22

23

24

25

26

27

28

29

30

31

32

33

34

35

36

37

38

39

40

41

42

43

44

45 **Abstract**

46 Nature-based solutions are attracting interest for their potential to enlist ecological processes as  
47 cost-effective and safe ways to capture and store carbon in forest ecosystems. Such solutions  
48 often need to be implemented in landscapes in which there are longer-established values for  
49 other ecosystem services including wildlife and timber production. Here we develop an  
50 integrative model that illustrates the inherent trade-offs that will arise among the competing  
51 values for landscape space and how to resolve them. The analysis characterizes boreal forest  
52 ecosystem dynamics involving interactions among the main trophic compartments of an intact  
53 boreal ecosystem, aka “nature”. The model accounts for carbon accumulation via biomass  
54 growth of forest trees (timber), carbon loss due to controls from moose herbivory that varies with  
55 moose population density (hunting), and soil carbon inputs and release, which together determine  
56 the carbon sink strength of the ecosystem. We link the ecological dynamics with an economic  
57 analysis by assigning a price to carbon stored within the intact boreal forest ecosystem. We then  
58 weigh these carbon impacts against the economic benefits of timber production and hunting  
59 across a range of moose population densities. Combined, this carbon-bioeconomic program  
60 calculates the total ecosystem benefit of a modelled boreal forest system, providing a framework  
61 for examining how different forest harvest and moose densities influence the achievement of  
62 carbon storage targets, under different levels of carbon pricing. The analysis shows that  
63 promoting nature-based solutions merely for carbon storage may result in loss of a key part of  
64 “nature” via loss of the trophic structure and key functional controls in the ecosystem.

65

66

67

## 68 INTRODUCTION

69 Nature-based solutions are attracting interest for their potential to enlist ecological processes as  
70 cost-effective and safe ways to mitigate and adapt to climate change, with the co-benefit that  
71 they could help to reverse biodiversity loss and protect ecosystems, along with their functions  
72 and services (Girardin et al., 2021; Miles et al., 2021; Mori, 2020; Osaka et al., 2021; Seddon et  
73 al., 2021, Smith et al., 2022). This is considered a win-win for protecting biodiversity and the  
74 climate. Indeed, the UN Convention on Biological Diversity Post-2020 Global Diversity  
75 Framework (CBD/WG2020/3/3) and the IPCC Sixth Assessment (IPCC 2022) actively promote  
76 nature-based solutions as being vital to reduce the risk of exceeding 2°C while sustaining both  
77 nature and human livelihoods.

78 Nature-based solutions are now attracting attention as financial investment opportunities in  
79 the form of carbon offsets to enhance atmospheric CO<sub>2</sub> uptake and storage in ecosystems (Busch  
80 et al., 2019; Chami et al., 2022; Kooijman et al., 2021; Girardin et al., 2021; Seddon et al., 2021).  
81 Carbon offset payments are further seen as ways to incentivize the protection of nature (i.e.,  
82 species, ecosystems, and ecosystem services) as part of a broader effort to create a sustainable  
83 nature-based economy. Forest ecosystems especially are considered to have high potential for  
84 investment owing to their capacity to capture and store large amounts of atmospheric CO<sub>2</sub> in  
85 plant biomass and in soils (Bastin et al., 2019; Busch et al., 2019; Fargione et al., 2018; Griscom  
86 et al., 2017; Houghton & Nassikas, 2018; McCarney et al., 2007; Salvatori & Pallante, 2021).  
87 Such investments are viewed as potentially having ancillary benefits for conservation by  
88 protecting habitat for a diversity of wildlife species (Buote et al., 2020; Littlefield & D'Amato,  
89 2021; McCarney et al., 2007; Rittenhouse & Rissman, 2012).

90 However, treating wildlife conservation merely as an ancillary benefit overlooks the

91 functional role of wildlife species in controlling forest ecosystem processes (Brodie & McIntyre,  
92 2019; Kielland & Bryant, 1998; Osuri et al., 2016; Pastor et al., 1988; Peres et al., 2016;  
93 Ramirez et al., 2021; Seagle, 2003; Sobral et al., 2017) including controlling the amount of  
94 carbon that is captured and stored (Brodie & Gibbs 2005; Berzaghi et al., 2019; Osuri et al.,  
95 2016; Peres et al., 2016; Sobral et al., 2017; Wilmers & Schmitz, 2016). Hence not accounting  
96 for these functional roles could lead to nature-based solutions failing to meet their carbon storage  
97 targets (Schmitz & Leroux, 2020; Schmitz et al., 2023), let alone overlooking the considerable  
98 economic value that comes from their functional controls over carbon capture and storage (Bello  
99 et al., 2021; Berzaghi et al., 2022; Brodie, 2018; Macias-Fauria et al., 2020).

100 We introduce here an approach for undertaking bioeconomic analyses of dynamic “nature” in  
101 support of nature-based carbon offsets. By dynamic nature, we mean both the species  
102 composition and functional interactions among species within and between trophic  
103 compartments of ecosystems that control ecosystem processes including carbon cycling. We  
104 illustrate our approach using boreal forests of the northern hemisphere as a case example. Boreal  
105 forests represent the largest forest biome globally and, after tropical forests, perhaps hold the  
106 largest global carbon-stores (Gauthier et al., 2015).

107 A dynamic boreal ecosystem can be minimally described as interactions among several key  
108 trophic compartments—soils, primary producers (trees), browsers of trees (moose), and  
109 predators of moose (wolves and humans) (Yona et al., 2018). These key ecosystem components  
110 influence boreal forest carbon dynamics via several natural control processes. Plants increase  
111 their biomass carbon by converting atmospheric CO<sub>2</sub> to new biomass, i.e., net primary  
112 productivity (NPP). As a key consumer of plant biomass, moose control NPP, and hence carbon  
113 capture and storage as biomass. The degree of control over NPP varies with moose abundance

114 and browsing intensity (Petersen et al., 2023; Wilmers & Schmitz, 2016). Wolves and humans in  
115 turn suppress moose populations. They thereby may indirectly augment carbon capture and  
116 storage by increasing NPP (Wilmers & Schmitz, 2016; Yona et al., 2018). As well, soil  
117 reservoirs store dead organic matter because cool soil conditions of intact boreal forests limit  
118 microbial decomposition rates and hence soil CO<sub>2</sub> release (Schmitz et al., 2003). Hence, boreal  
119 soils, perhaps even more than trees, play a large role in the total carbon balance of the boreal  
120 ecosystem (Bradshaw & Warkentin, 2015).

121 Despite helping to augment carbon capture and storage, wolves are being culled in many parts  
122 of the boreal forest to meet specific values for conserving other threatened wildlife species that  
123 are vulnerable to wolf predation (Hebblewhite, 2017; Maher et al., 2020). This reflects a  
124 willingness of managers to overlook the need to take a holistic perspective that considers the  
125 functional roles of animals in their entirety. In a more holistic context, the release from predation  
126 pressure could cause moose populations to increase and heavily browse growing trees, thereby  
127 changing tree species composition and biomass across the landscape (Jaeger et al., 2017). Heavy  
128 browsing, especially of regenerating trees, reduces forest canopy height and closure and causes  
129 soil warming (Bonan, 1992; Kielland & Bryant, 1998; Schmitz et al., 2003) resulting in lower  
130 humidity, warmer and drier soils, and hence CO<sub>2</sub> release via increased soil microbial respiration  
131 (Crowther et al., 2016) or increased frequency and intensity of forest fires (Schmitz et al., 2003).  
132 Thus, failing to account for moose effects when taking measures to conserve other wildlife in  
133 this ecosystem could lead to conflicts with carbon offset investments. In addition, large scale and  
134 widespread timber extraction is an essential source of economic and social welfare of local  
135 communities (Yona et al., 2018). Rising moose abundances, consequent to wolf culling, could  
136 reduce timber production as well (Schmitz, 2005; Wam et al., 2005). But moose cannot be

137 eliminated from the landscape entirely to avoid negative impacts on timber production or carbon  
138 storage. This is because the species is valued by local communities for providing hunting  
139 opportunities and provisioning and social and cultural services (Bélisle et al., 2021; Natcher  
140 2009; Timmerman & Rogers, 2005; Wam et al., 2005).

141 Hence, sustaining a boreal nature-based economy for these different values requires treating  
142 the three sectors—wildlife, timber and carbon—in a functionally integrated way, yet they  
143 currently are not (Chapin & Whiteman, 1998; McCarney et al., 2007; Yona et al., 2019). Here  
144 we illustrate how to undertake such an integrative, ecologically informed functional examination  
145 to reveal the economic benefits and opportunity costs of explicitly managing the interplay and  
146 trade-offs among the different trophic compartments of the boreal ecosystem. This entails  
147 consideration beyond mere existence value of moose (Krutilla, 1967) to account for their  
148 functional role as drivers of economic return via impacts on timber production, via impacts on  
149 forest carbon uptake and storage in tree and soil biomass, and via hunting revenue. While the  
150 additional provisioning and cultural services (Bélisle et al., 2021; Natcher 2009; Timmerman &  
151 Rogers, 2005; Wam et al., 2005) could also be considered in bioeconomic analyses (e.g.,  
152 Ansuategi et al., 2019; Armstrong et al., 2017; Enriquez & Finnoff, 2021), our focus on moose  
153 foraging and hunting impacts on ecosystem carbon capture and storage carbon is intended to  
154 highlight the underappreciated fact that moose management can change the direct impact of  
155 moose on whole ecosystem functionality and hence on key regulatory and provisioning  
156 ecosystem services of boreal forests.

157 Our analysis considers the three-way interaction between (i) managing for forest carbon  
158 sequestration and storage in tree and soil biomass vs (ii) managing for tree biomass carbon  
159 removal from timber harvest vs (iii) managing for tree biomass carbon removal and alteration of

160 soil processes arising from changes in moose abundance, and hence browsing impacts. The key  
161 insight from our analysis is that rising carbon prices can incentivize significant alteration of  
162 dynamic nature via large reductions in moose population density to ensure the maximization of  
163 the benefit of the nature-based solution. This arises because a carbon market can quickly provide  
164 an income stream that becomes far larger than any revenue from hunting or other ecosystem  
165 service values for moose. This can in turn create issues about the fairness of wealth distribution  
166 among local communities living within boreal forests.

167 The insights we offer have potentially significant, broad scale implications given that  
168 geographically boreal forests of northern Canada and Russia cover 10 percent of the earth's land  
169 area. While our examination here focuses on boreal forest ecosystem dynamics, the principles  
170 can be generalized to other forests ecosystems, and indeed other ecosystems globally. Hence, our  
171 analysis, while examining a case study, is also intended to offer conceptual insight into ways of  
172 integrating climate policy with wildlife and forest and ecosystem management more broadly.

173

## 174 **THE MODEL**

175 Previous analyses of the interplay between boreal forest timber, carbon and moose have either  
176 treated moose and other wildlife indirectly via the ancillary benefits arising from conserving and  
177 enhancing wildlife habitat while managing for tree biomass carbon (e.g., McCarney et al., 2008),  
178 or directly as a consumer of harvestable timber production (Wam et al., 2004). Here we expand  
179 the scope of analysis using an ecosystem dynamics model that accounts for moose functional  
180 control not only over timber production but also over carbon uptake and storage in tree biomass  
181 and in soils. The modeling explores two baseline scenarios for forest harvesting and associated  
182 forest productivity (carbon capture) and standing timber biomass carbon: a "non-harvested"

183 system (i.e., no timber is harvested) and a “harvested forest” system (i.e., timber is harvested).  
184 For each scenario we consider how moose will impact forest productivity and timber biomass  
185 carbon at varying moose harvest (hunting) levels. Together timber x moose harvesting scenarios  
186 create different conditions on which to apply a carbon market. The analyses reveal how  
187 ecosystem functioning in the presence and absence of timber and moose harvest alter the carbon  
188 content of the forest ecosystem. This allows an examination of how different carbon prices  
189 could alter the abundance and trophic structure of the ecosystem.

190 The following presents a conceptual overview of our modeling. Details of model  
191 calibrations and numerical implementation are presented in the Appendix S1. A key element of  
192 our approach is that we solve for the “social planner’s” solution in different scenarios. One can  
193 interpret this as the manager’s solution that seeks to optimize the overall net benefits among the  
194 sectors considered. While this means we do not account for strategic incentives among sectors  
195 that might arise (i.e., moose hunting, timber harvesting, and the carbon market), it does enable us  
196 to focus on tradeoffs that arise with coordinated management of the ecological and forest  
197 management system as a whole.

198

### 199 **The ecological system**

200 The structure of our model boreal ecosystem is characterized as interactions among four  
201 functional trophic levels—soil, primary producers (trees), browsers of trees (moose), and hunters  
202 of moose (wolves or humans)—that comprise a food chain in which each trophic level controls  
203 the others’ population (Schmitz, 2005). To model forest carbon dynamics, we modify a simple  
204 dynamical systems model describing trophic interactions (Schmitz, 1992) to dynamically link  
205 forest tree production with the moose population and soil organic matter pool. Tree biomass,



206 moose density and soil carbon pool size are treated as dynamic state variables. We treat hunter  
 207 abundance as a fixed control variable, in light of management that sets fixed hunter harvest  
 208 levels of moose or the abundance of wolves present in the ecosystem. Our analyses models  
 209 biomass dynamics in tonnes of biomass per square km ( $t/km^2$ ) in the ecological systems and then  
 210 converts biomass to biomass carbon ( $tC/km^2$ ) in the economic system. The ecosystem dynamics  
 211 are described by three fundamental equations:

212

$$213 \quad \frac{dT}{dt} = \mathcal{F}_T(T) - \mathcal{F}_M(T)M - H_T - \rho T \quad (1)$$

$$214 \quad \frac{dM}{dt} = [\varepsilon \mathcal{F}_M(T) - d_M - \Lambda M]M - H_M \quad (2)$$

$$215 \quad \frac{dOM_t}{dt} = \rho T + d_M M + \pi H_T - m_S OM. \quad (3)$$

216

217 where  $T$  is standing tree biomass ( $t/km^2$ ),  $M$  is moose density ( $animals/km^2$ ),  $OM$  is the soil  
 218 organic matter pool ( $t/km^2$ ), and all other terms are defined as follows.  $\mathcal{F}_T(T)$  represents the net  
 219 biomass growth rate of trees or net primary productivity (NPP = carbon uptake – carbon  
 220 respiration:  $t/km^2 \cdot yr$ ) before other sources of biomass loss. These other losses include moose  
 221 consumption of tree biomass  $\mathcal{F}_M(T)$  ( $t/km^2 \cdot animal \cdot yr$ ) which varies functionally with tree  
 222 biomass at a per capita rate, timber harvesting rate  $H_T$  ( $t/km^2 \cdot yr$ ), and loss of dead biomass to  
 223 the  $OM$  pool as natural detrital inputs at rate  $\rho T$  ( $t/km^2 \cdot yr$ ). Changes in moose population  
 224 abundance results from consumption and assimilation of plant biomass to meet physiological  
 225 needs for maintenance and reproduction  $\varepsilon \mathcal{F}_M(T)$ , where  $\varepsilon$  (%) is the efficiency by which moose-  
 226 consumed plant biomass is assimilated and converted into per capita moose growth and  
 227 reproduction,  $d_M$  is the per capita natural mortality rate of moose ( $\%/ km^2 \cdot yr$ ),  $\Lambda M$  is a rate cost  
 228 of density-dependent interactions among members of the moose population ( $\%/ km^2 \cdot animal \cdot$   
 229  $yr$ ), and  $H_M$  ( $animals/km^2 \cdot yr$ ) is the hunter harvest rate of moose.  $OM$  dynamics are a function

230 of buildup due to detrital inputs from trees  $\rho T$ , death and decay of moose  $d_M M$ , debris inputs  
231 from timber harvesting  $\pi H_T$ , and loss due to soil respiration  $m_S OM$ .

232

### 233 **Forest management system**

234 We consider two scenarios for timber harvesting. The first assumes a “non-harvested” system  
235 (i.e., no timber is harvested) such that  $H_T = 0$ . This scenario assumes an average stand age of  
236 100 years (McCarthy & Weetman, 2006; McLaren & Peterson, 1994). The second scenario, the  
237 “harvested forest” system (i.e., timber is harvested), assumes that a constant fraction of the  
238 standing tree biomass is harvested in each time period, where the fraction harvested depends on  
239 an assumed rotation length of  $r$  years. We express annual timber harvest as a function of the  
240 standing biomass and the assumed rotation length such that  $H_T = H_T(T; r)$ . The assumption of a  
241 fixed rotation length is a simplification of practices in the forestry sector, but one that enables us  
242 to focus primarily on the ecological interactions. We assume that forests are composed of spruce  
243 and pine and harvested as even-aged stands, in accordance with common boreal forestry  
244 practices (Asante et al., 2011). For boreal stands harvested without a carbon market, a harvest  
245 rotation of 80 years tends to be the ideal mature stand age for clear-cutting (Asante et al., 2011).  
246 Thus, a rotational harvest management program that removes and regenerates  $1/80^{\text{th}}$  of the entire  
247 forest area each year within an 80-year time frame ensures steady annual revenues (Asante et al.,  
248 2011). This program lead us to model dynamics for 80 uneven-aged forest plots, aged in discrete  
249 one-year increments. We use the TIPSY forest biomass simulator and Chapman Richards  
250 functions (Asante et al., 2011) to estimate annual timber harvest for the  $1/80^{\text{th}}$  rotational harvest  
251 program in the absence of moose.

252

## 253 **The economic system**

### 254 Analytical Approach

255 In what follows, we assume that moose hunting harvest level, and in turn moose density, is the  
256 choice variable such that for any choice of  $M$ , we can define the steady state conditions. We then  
257 compare steady-state conditions between incremental changes in moose abundance rather than  
258 on the transitional dynamics from one steady state to another, or following disturbances such as  
259 wild fires. We define a steady state as a condition where the standing tree biomass and moose  
260 population are constant. That is, Eqs. 1 and 2 are equal to zero. We do not assume that Eq. 3 will  
261 equal zero, reflecting the more realistic possibility for organic matter to continually increase over  
262 time, even if  $T$  and  $M$  are constant. This means that setting  $dT/dt = dM/dt = 0$ , along with one  
263 of the timber harvesting conditions (non-harvested or harvested), establishes a system of two  
264 equations and three unknowns:  $T$ ,  $M$ , and  $H_M$ .

265 A steady state is therefore fully defined by the functions  $\hat{T}(M)$  and  $\hat{H}_M(M)$ , which are  
266 implicitly defined by Eqs. 1 and 2. As described above, a non-harvested forest imposes the  
267 constraint  $H_T = 0$ , whereas the harvested forest sets  $H_T = H_T(\hat{T}(M); r)$ . Finally, note that given  
268 a steady state,  $dOM_t/dt$  changes over time depending on the steady-state values and an initial  
269 value of  $OM$ . This is discussed further below.

270

### 271 Baseline Equilibria

272 We establish two baseline conditions before introducing the possibility of payments for carbon  
273 sequestration. The first assumes that the forest is non-harvested and the chosen level of  $M$  is  
274 intended to maximize the net financial benefits of moose hunting alone. The second assumes the  
275 forest is harvested and considers the dual objective of choosing  $M$  to maximize the combined net

276 financial benefits to hunting and timber harvesting. These become the baselines upon which we  
 277 subsequently add a carbon market.

278 We first specify the net financial benefits (i.e., benefit minus costs) of each activity. Let  
 279  $NB_{H_M}(H_M)$  denote the net benefits of moose hunting, and let  $NB_{H_T}(H_T)$  denote the net benefits  
 280 of timber harvesting. Assuming the forest is non-harvested and the level of moose density is  
 281 chosen with only human hunters in mind, the steady state, chosen level of moose density will  
 282 satisfy

$$283 \quad M^\circ = \arg \max_M \{NB_{H_M}(\hat{H}_M(M)): H_T = 0\}, \quad (4)$$

284 where the constraint clarifies that timber harvest must equal zero. Now assuming the level of  
 285 moose density is chosen to maximize the net benefits to both hunters and timber harvesters, the  
 286 solution will satisfy

$$287 \quad M^{\circ\circ} = \arg \max_M \{NB_{H_M}(\hat{H}_M(M)) + NB_{H_T}(\hat{H}_T(M))\}. \quad (5)$$

288 The maximand in (5) differs from (4) because it includes the net benefits of timber harvesting,  
 289 which is no longer restricted to zero. In particular, the second optimization accounts for the way  
 290 that moose density affects the steady-state timber harvest. Because  $\hat{H}_T(M)$  always decreases with  
 291  $M$  (that is, a larger moose population means less harvestable timber in the steady state),  
 292 accounting for the timber harvest in moose management will always create an incentive for  
 293 lower moose density, i.e.,  $M^\circ > M^{\circ\circ}$ . The net benefit of moose harvesting is also density  
 294 dependent itself; benefit per moose generally increases as moose density decreases (see  
 295 additional details in Appendix S1).

296

297 Biomass Carbon

298 Central to our analysis is the introduction of payments for carbon sequestration in trees and soils.  
299 We therefore need a measure of the carbon content in  $T$  and  $OM$ . Our basic characterization of  
300 forest ecosystem dynamics abstracts considerable detail found in many current carbon cycle  
301 models that explicitly account for variation in the carbon content of trees due to fluxes and  
302 storage among finely divided ecosystem biomass compartments (e.g., wood, leaves, roots) and  
303 due to varying availability of soil nutrients and water. Furthermore, current carbon cycle models  
304 characterize carbon flux at explicitly physiological levels including photosynthesis, and plant and  
305 soil respiration (Holmberg et al., 2019; Piao et al., 2013; Zaehle et al., 2014.). While such  
306 mechanisms can be embedded in Eqs. 1 and 3 (Schmitz & Leroux, 2020), specifying this level of  
307 detail would add unnecessary complexity given the purpose of analysis here, which is to  
308 illustrate how to examine trade-offs that account for the dynamical role of animals on carbon  
309 exchange and storage, rather than estimate actual carbon storage for a particular region. We  
310 therefore assume, as a first approximation, that carbon photosynthetically fixed in trees is a  
311 constant fraction  $\alpha = 0.5$  of live biomass  $T$  and dead organic matter  $OM$  from trees (Houghton et  
312 al., 2009; Jain et al., 2010). In natural ecosystems, the amount of soil carbon storage varies  
313 spatially. However, for the purposes here, we do not consider spatial variations in our modeled  
314 ecosystem. Instead we assume a starting condition of 34,000 tC per km<sup>2</sup> to reflect average values  
315 found across boreal forest landscapes (Watson et al., 2000).

316

### 317 Carbon Payments

318 We consider a market for carbon sequestration where payments are based only on the additional  
319 carbon stored due to changes in the control variable  $M$ . We assume a price of carbon dioxide  
320 denoted  $P_C$ , and this is translated into a price of carbon via  $\delta P_C$ . As noted previously, carbon is

321 stored in two places relevant for our analysis: trees and soils in quantities  $\alpha T$  and  $\alpha OM$ ,  
 322 respectively.

323 Carbon payments for storage in trees are assumed to take the following form:

$$324 \quad f(M; \bar{M}) = \frac{\delta P_c \alpha}{r} (\hat{T}(M) - \hat{T}(\bar{M})), \quad (6)$$

325 where  $M$  is any chosen level of moose density, and  $\bar{M}$  is a corresponding baseline for  
 326 comparison, before the introduction of a carbon price (see below). The carbon payments are  
 327 therefore structured to compensate for the difference in standing carbon between two steady  
 328 states, where the payment is put on an annual basis depending on the assumed rotation length  $r$ .  
 329 This means that the forest carbon market is structured to pay for storage over the length of a  
 330 rotation, for which we have annualized the payments.

331 Carbon payments for the additional increment of soil carbon are similarly structured to  
 332 compensate for the difference arising between two steady states. But at equilibrium, there is no  
 333 change in steady state standing biomass ( $dT/dt = 0$  in Eq. 1), while soil carbon may be  
 334 continuously accruing ( $dT/dt \neq 0$  in Eq. 3). Therefore, whereas payments for forest carbon ( $f$   
 335 ( $M; \bar{M}$ )) compensate for a discrete change in the total storage level, soil carbon payments  
 336 represent a change in the *rate* of soil accumulation. This difference occurs because soil carbon  
 337 can continuously accrue across timber generations, while a shift in the steady-state standing  
 338 biomass carbon only occurs once across the timber rotation generation.

339 Defining this payment similarly requires quantifying the annual changes in soil carbon  
 340 across the timber rotation period, given the spatial heterogeneity of carbon additions and  
 341 decomposition across the rotation. We define this payment by first solving for  $OM_t$  for any  
 342 period  $t = 1, 2, \dots, r$  given an initial rate of soil carbon accumulation  $OM_0$ :

$$343 \quad OM_t(M; OM_0) = \rho \hat{T}(M) + d_M M + \pi \hat{H}_T(M) - m_S OM_{t-1}. \quad (7)$$

344 which determines the amount of loss due to decomposition during the rotation in relation to  
 345 existing OM storage rate (note: higher levels of starting OM lead to more carbon lost during  
 346 forest harvesting, and more loss potential if high moose populations trigger decomposition).  
 347 Now, given assumptions about the initial values of  $OM_0$  and a baseline steady-state equilibrium,  
 348 we define the soil carbon payment as follows:

$$349 \quad k(M; \bar{M}) = \frac{\delta P_C \alpha}{r} \sum_{t=1}^r [OM_t(M; OM_0) - OM_t(\bar{M}; \bar{OM}_0)]. \quad (8)$$

350 The summand adds up the difference in organic matter accrual over all  $r$  time periods (by taking  
 351 the difference between the change in each period from the baseline over  $r$  years), multiplying by  
 352  $\alpha/r$  converts the total difference into an average, annual carbon difference, and  $\delta P_C$  translates  
 353 the quantity into a carbon payment for the change in the rate of  $OM$  storage. This average annual  
 354 carbon accrual across  $r$  rotation plots means that payments for soil carbon are structurally  
 355 different from forest carbon payments;  $k$  represents annual average additional carbon storage  
 356 between  $M$  and  $\bar{M}$ , while  $f$  utilizes  $r$  to annualize payments for the one-time change in  $T$  storage  
 357 between  $M$  and  $\bar{M}$ .

358

### 359 Equilibria with Carbon Payments

360 We now consider how the non-harvested and harvested steady state equilibria change with the  
 361 introduction of a carbon payment. With our setup, the first step is to consider how the conditions  
 362 differ for the optimally chosen level of moose density.

363 The non-harvested forest level of moose density with a carbon payment will satisfy

$$364 \quad M^* = \arg \max_M \{NB_{H_M}(\hat{H}_M(M)) + f(M; M^\circ) + k(M; M^\circ): H_T = 0\}. \quad (9)$$

365 where (9) differs from (4) because the carbon payments enter the maximand, and importantly,  
 366 the baseline condition upon which the payments are calibrated to the solution  $M^\circ$  in (4). To the

367 extent that greater moose density leads to less standing carbon and less accumulated soil carbon,  
 368 we would expect moose densities to be lower with the carbon payment, that is,  $M^* < M^\circ$ .  
 369 Moreover, using the different terms in (4) and (9), we can solve explicitly for the carbon  
 370 payments (for trees and soil) and the change in net benefits to moose hunters.

371 The choice of moose density with a harvested forest and carbon payments will satisfy

$$372 \quad M^{**} = \max_M \{NB_{H_M}(\hat{H}_M(M)) + NB_{H_T}(\hat{H}_T(M)) + f(M;M^\circ) + k(M;M^\circ)\}.(10)$$

373 In this case, and in parallel, (10) differs from (5) because the carbon payments are included, and  
 374 the baseline condition for calibrating the payments to the solution  $M^\circ$  in (5). It follows that (10)  
 375 introduces added incentives, compared to (9), to reduce moose density for purposes of greater  
 376 benefits from timber harvesting.

377 Deriving analytical solutions for the bioeconomic system is challenging given the number of  
 378 equations involved and their inherent nonlinearities. We therefore conduct the analyses  
 379 numerically. Our approach involves examining carbon dynamics across gradients of moose  
 380 population density as managed through moose hunting. The numerical analysis thus examines  
 381 carbon dynamics in terms of steady-state conditions that permit expressing each of the  
 382 endogenous variables ( $T$ ,  $M$  and  $OM$ ) as functions of the other variables and moose and timber  
 383 harvesting levels to conduct a carbon accounting of the boreal ecosystem. Detailed explanation  
 384 of the model functions and numerical analyses is presented in Appendix S1.

385

## 386 RESULTS

387 The numerical analysis reveals that under non-harvested forest conditions (intact nature), the  
 388 levels of standing tree biomass, NEP, and timber harvested all decrease in a sigmoid manner  
 389 with increasing moose density (Figure. 1). This nonlinear trend between moose abundance and



390 the three response variables is a consequence of an interplay between two intra-moose  
391 population controls that together determine levels of moose impacts (Appendix S1 Eq. S2, S5).  
392 One control comes from density-dependent negative feedback on moose population growth with  
393 rising moose density (i.e., logistic moose population growth), and a second control comes from a  
394 saturating rate of moose biomass consumption with increasing tree biomass (i.e., a saturating  
395 Type II moose functional response). However, the dominance of each control changes across the  
396 moose density gradient. At low moose densities (high plant biomass) moose are unable to cause  
397 heavy damage to plants because their consumption of plant biomass is saturated. At high moose  
398 densities (low plant biomass) moose again are unable to increase damage to plants because of  
399 strong intra-population competition for plant biomass. Hence, the strongest moose impacts occur  
400 at intermediate moose densities when there is a transition between the dominance of one control  
401 to the other. Accordingly, over low but increasing moose densities, moose will have neutral to  
402 minor negative impacts on high forest biomass and NEP. As moose densities rise to intermediate  
403 densities, the system over time will undergo a quasi-threshold change in which plant biomass  
404 and NEP decline rapidly (Figure 1). This is followed again by neutral or minor negative impacts  
405 on low forest biomass and NEP high moose densities. This modeling reveals that a rise in moose  
406 density from 0.5 to 1.0 animals per km<sup>2</sup>, which is at the lower end of recorded moose densities  
407 for boreal forests (Jensen et al., 2020; Petersen et al., 2023), is sufficient to reduce carbon storage  
408 in soil organic matter by 25 percent. This modeled reduction in carbon storage is consistent with  
409 previous empirical estimates (Schmitz et al., 2014, Wilmers & Schmitz, 2016) and remote  
410 sensing analyses of forest productivity in relation to moose densities across North American and  
411 Scandinavian boreal forests (Petersen et al., 2023).

412 The ecological control by moose on forest standing tree biomass, NEP, and timber available  
413 for harvest leads to nonlinear relationships between carbon pricing and the optimal level of  
414 moose density for non-harvested ( $M^*$ ) and harvested ( $M^{**}$ ) forest scenarios in Eqs. 9 and 10. In  
415 the absence of a carbon payment (the Y-intercept of each curve), moose density is solely driven  
416 by benefits from hunting (Figure 2, red lines) and the combination of benefits from hunting and  
417 timber harvest (Figure 2, blue line). In the absence of carbon pricing, optimal moose density in  
418 the harvested scenario is between 0.33 and 0.66 times lower than the non-harvested scenario due  
419 to balancing the trade-off in benefits from moose and timber harvesting.

420 Adding a carbon market would encourage lowering moose densities to maximize forest  
421 carbon storage. The amount of decline in density needed to maximize carbon storage varies in a  
422 negative exponential manner with rising carbon prices, with the trend in decline remaining  
423 similar for different initial harvested optimal moose equilibrium density ( $M^o = 1.0$ , and  $M^o$   
424  $= 0.5$ ). This need for a rapid managed decline in moose density results from the high marginal  
425 change in forest carbon-impact of moose browsing at population densities between 0.5 to 1.0  
426 moose per km<sup>2</sup>, weighed against the comparatively low marginal benefit of the additional  
427 sustained moose harvest yield. The analysis reveals that as the carbon price increases, the  
428 benefit-maximizing moose population density in non-harvested and harvested forests converge to  
429 a very low moose density between 0.1 and 0.2 per km<sup>2</sup> because carbon benefits progressively  
430 outweigh benefits from the other sectors. That is, rising carbon prices encourage large reductions  
431 in moose population density to ensure the maximization of carbon storage in the ecosystem.  
432 Indeed, carbon prices as low as \$5 per tCO<sub>2</sub>, would already encourage a major 50% reduction in  
433 optimal moose density (Figure 2). Moose density between 0.1 and 0.2 per km<sup>2</sup> represents the  
434 point beyond which further moose population reduction would have limited impact on ecosystem

435 carbon storage (see Figure 1), i.e., moose are no longer a functionally significant player in the  
436 ecosystem.

437 In the non-harvested forest, the reductions in optimal moose density with increasing carbon  
438 price translates into a nonlinear saturating increase in total carbon stored in tree biomass and  
439 annual soil OM carbon accumulation with increasing carbon price. It increases only slightly and  
440 linearly in the harvested forest (Figure 3). This saturation results from constraints imposed by  
441 underlying ecosystem dynamics. But the absolute difference in carbon storage in trees between  
442 non-harvested and harvested cases results from less carbon stored in the average younger-aged  
443 trees comprising stands in the 80-year rotation of the harvested forest. The difference in annual  
444 OM storage results primarily from the decomposition that occurs in younger forest plots  
445 triggered by forest harvesting. The small increase in carbon storage with increasing carbon price  
446 in the harvested forest arises because the system is already optimized for both moose and timber  
447 harvesting before the introduction of carbon prices. This stems from the moose population  
448 decreasing less in the harvested forest as carbon price increases than in the non-harvested forest.  
449 Hence, perverse effects of carbon pricing on the destruction of nature become more of a concern  
450 in non-harvested systems because harvested systems already have an incentive to lower the  
451 moose population.

452 The financial benefits of moose hunting and carbon storage vary inversely with increasing  
453 carbon price (Figure 4). This is because the decline in moose population density with increasing  
454 carbon prices (see Figure 2) results in greater tree and soil carbon benefits (a function of both the  
455 increasing level of carbon storage and the increasing price per unit of carbon stored), and a  
456 reduction in moose hunting benefits. The differences in the amount of benefit between the non-  
457 harvested and harvested forest results from moose populations shifting more substantially in the

458 non-harvested forest case (see Figure 2), with a concomitant larger reduction in hunting benefits  
459 and a greater change in forest carbon composition than in the harvested forest (Figure 4).

460

## 461 **DISCUSSION**

462 There is growing interest to account for the economic value of nature-based solutions that  
463 capture and store carbon in ecosystems (Chami et al., 2022). This includes financially accounting  
464 for carbon benefits accrued via the conservation of animals to preserve their functional roles that  
465 control the carbon cycle in ecosystems (e.g., frugivory and dispersal of seeds from carbon dense  
466 trees [Brodie, 2018; Bello et al., 2021; Berzaghi et al., 2022]; trampling and foraging to restore  
467 and protect plant production in the arctic steppe and carbon in permafrost [Macias-Fauria et al.,  
468 2020]). In some cases, valuing the animal effects involves a straightforward calculation of the  
469 additional carbon accrued with every unit of the animal population increase (Bello et al., 2021;  
470 Macias-Fauria et al., 2020). In other cases, animal effects on carbon storage may vary  
471 nonlinearly with animal abundance (Brodie, 2018; Berzaghi et al., 2019) such that over a range  
472 of low to intermediate density animals could have neutral or beneficial effects with a switch to  
473 negative effects at high density (Berzaghi et al., 2019; this study). Hence considering wildlife  
474 conservation to meet the dual goals of mitigating biodiversity loss and climate mitigation must  
475 go beyond a focus merely on protecting and restoring species, and explicitly include  
476 consideration of their density-dependent population ecological effects on ecosystem processes  
477 (Fig. 1).

478 Our analysis highlights potential risks associated with promoting forest production  
479 merely as a nature-based solution for carbon capture and storage (Bastin et al. 2019; Fargione et  
480 al., 2018; Griscom et al., 2017; Houghton & Nassikas 2018). This need to consider risks will be

481 especially critical whenever new carbon offset programs are superimposed onto landscapes in  
482 which there are longer-established values for other ecosystem services. In boreal forest  
483 ecosystems for instance, this could include forest production of timber for extraction (Holmberg  
484 et al., 2019; McCarney et al., 2007; Wam et al., 2005, Yona et al., 2019), provisioning and  
485 cultural services provided by wildlife tourism and hunting (Bélisle et al., 2021; Holmberg et al.,  
486 2019; Timmerman & Rodgers 2005) and conservation of threatened wildlife species (Drever et  
487 al., 2019). The consideration of the functional roles of animals in these ecosystem services may  
488 require reconciling trade-offs because of the different ecosystem service values provided by any  
489 given animal species (Brodie, 2018).

490 Our analysis for moose reveals that failing to anticipate and reconcile such conflicts may  
491 result in loss of a key part of “nature” vis à vis loss of the trophic structure and key functional  
492 controls within the ecosystem to maximize carbon storage. The risk of this outcome increases  
493 with increasing prices of carbon. This is because maximizing ecosystem carbon storage with  
494 increasing carbon prices would necessarily incentivize reducing moose population size  
495 substantially due to moose limitation of forest biomass production and hence carbon uptake and  
496 biomass storage capacity. This reduction could become especially profound in the non-harvested  
497 scenario, where moose population sizes have not yet been optimized to support timber  
498 production (Figure 2).

499 Regardless of scenario, superimposing a carbon market onto a harvested or non-harvested  
500 forest landscape could collapse the moose hunting economy. This is because even at a low  
501 carbon price, the benefit for moose hunting would become increasingly negative as carbon price  
502 increases (Figure 4) because moose populations must be reduced to such an extent that sustaining  
503 hunting comes at a net cost. Consequently, the welfare of a community dependent on the

504 recreational and cultural services provided by moose could become increasingly jeopardized by  
505 carbon offset investments. This provides a specific example where managing natural systems  
506 primarily to reduce atmospheric CO<sub>2</sub> emissions might have perverse effects on natural systems  
507 themselves and raise questions about distributional fairness (Honegger et al., 2021). But moose  
508 population management is typically accomplished through hunting, and so without hunting it  
509 may be challenging to meet carbon storage goals of offset investments due to the need to  
510 implement carbon management initiatives predicated on reducing density of browsing species.

511         The solution to meeting the multiple objectives of management for wildlife, timber and  
512 carbon sequestration is to utilize hunting not just for game or recreation, but as part of a nature-  
513 based solution via a new means to enhance carbon sequestration (Yona et al., 2019). Doing so  
514 requires moving away from setting hunting levels using classic population-based maximum  
515 sustained yield (MSY) bioeconomic concepts to more holistic forest ecosystem dynamic  
516 bioeconomic concepts that set moose sustained yield to reach ecologically meaningful densities  
517 for carbon capture and storage (Schmitz & Sylvén, 2023). The determination of what is  
518 ecologically meaningful requires balancing moose density-dependent impacts on tree production  
519 and soil carbon deposition (Fig. 1) against carbon gains accrued in tree biomass and soil (Fig. 3).  
520 For the conditions (diminishing returns curves) specified in our modeling scenarios, ecologically  
521 meaningful becomes a density between 0.2 and 0.4 moose per square kilometer, which is much  
522 lower than the classic population-based MSY of 1 moose per square kilometer (Supplemental  
523 Appendix).

524         The much lower moose density leads to a loss of economic return to the hunting  
525 economy. But the amount of that loss, which increases with increased carbon price, can be  
526 imputed as the minimal cost of sustaining an intact forest for moose carbon and timber

527 production. This implies that rather than hunters paying for the opportunity to hunt moose,  
528 carbon offset investments should pay hunters for the service provided to sustain the nature-based  
529 climate solution along with other ecosystem services. That is, hunting can be viewed as a control  
530 on ecosystem dynamics much like the control exerted by wolves. Hence, an alternative way to  
531 value wolves is to quantify the economic benefit they provide to offset carbon programs via their  
532 control over moose populations (Schmitz et al., 2014). This could conceivably be imputed in the  
533 same way as the determination of the economic value of moose hunting.

534 Our ecosystem model is a basic caricature of ecosystem dynamics. As such it does not  
535 include an explicit account of biogeochemical processes in terms of carbon and nutrient  
536 dynamics that are characteristic of conventional models of ecosystem service production and  
537 carbon dynamics (Holmberg et al. 2019; Piao et al., 2013; Zaehle et al. 2014) as well as models  
538 that account for animal effects on biogeochemical processes driving carbon cycling (Rizzuto et  
539 al., 2024). This was done because our primary intention was to motivate new modeling  
540 developments by illustrating how an integrative approach can help us devise creative alternative  
541 solutions for climate change mitigation.

542 Thus, our modeling results do not offer estimates of carbon sequestration on which to  
543 base specific on-the-ground management decisions. Rather, our modeling approach offers  
544 insights on how to go about providing an integrative way to illustrate and quantify the trade-offs  
545 among different values and ecosystem services offered by forest ecosystems. Accurately  
546 accounting for carbon dynamics in nature-based solutions will require the development of new  
547 kinds of management models to capture the harvest and carbon implications of ecosystem co-  
548 uses. These models will need to explicitly blend classic animal and plant population density and  
549 production concepts with ecosystem trophic dynamic models that account for biogeochemical

550 cycling, production and net ecosystem carbon storage. Moreover, solutions for such models will  
551 need to move away from considering steady-state conditions, as is done in conventional forest  
552 management, to focus on transitions between steady states to anticipate outcomes of  
553 management for multiple different ecosystem values within a single ecosystem. Such new ways  
554 of analyzing the models will help to appropriately value different ecosystem components to  
555 avoid the perverse outcomes encountered in our current modeling in which implementing well-  
556 intentioned nature-based climate solutions could end up destroying dynamic nature.

557

#### 558 **ACKNOWLEDGMENTS**

559 This study was supported by funds from the Yale School of the Environment to OJS and MJK.

560

#### 561 **AUTHOR CONTRIBUTIONS**

562 JU, MJK and OJS conceived and designed the study. JU lead the model development and  
563 analyses in consultation with MJK and OJS. JU, MJK and OJS wrote the manuscript.

564

#### 565 **CONFLICT OF INTEREST STATEMENT**

566 The authors declare no conflicts of interest.

567

#### 568 **ORCID**

569 *Matthew Kotchen* <https://orcid.org/0000-0002-0350-6598>

570 *Oswald Schmitz* <https://orcid.org/0000-0003-1515-2667>

571

#### 572 **REFERENCES**



- 573 Ansuategi, A.D., D. Knowler, T. Schwoerer, and S. García-Martínez. 2019. “Local Fishing  
574 Communities and Nature-Based Tourism in Baja, Mexico: An Inter-sectoral Valuation of  
575 Environmental Inputs.” *Environmental and Resource Economics* 74:33–52.  
576 <https://doi.org/10.1016/j.jeem.2021.102441>
- 577 Armstrong, C.W., V. Kahui, G.K. Vondolia, M. Aanesen, and M. Czajkowski. 2017. “Use and  
578 Non-Use Values in an Applied Bioeconomic Model of Fisheries and Habitat  
579 Connections.” *Marine Resource Economics* 32:351–369. <https://doi.org/10.1086/693477>
- 580 Asante, P., G.W. Armstrong, and W.L. Adamowicz. 2011. “Carbon Sequestration and the  
581 Optimal Forest Harvest Decision: A Dynamic Programming Approach Considering  
582 Biomass and Dead Organic Matter.” *Journal of Forest Economics* 17: 3–17.  
583 <https://doi.org/10.1016/j.jfe.2010.07.001>.
- 584 Bastin, J.-F., Y. Finegold, C. Garcia, D. Mollicone, M. Rezende, D. Routh, C. Zohner, and T.  
585 Crowther. 2019. “The Global Tree Restoration Potential.” *Science* 365: 76-79.  
586 <https://doi.org/10.1126/science.aax0848>.
- 587 Bélisle, A.C., A. Wapachee, and H. Asselin. 2021. “From Landscape Practices to Ecosystem  
588 Services: Landscape Valuation in Indigenous Contexts.” *Ecological Economics* 179:  
589 106858. <https://doi.org/10.1016/j.ecolecon.2020.106858>.
- 590 Bello, C. L. Culot, C. Augusto, and M. Galetti. 2021. “Valuing the Economic Impacts of Seed  
591 Dispersal Loss on Voluntary Carbon Markets.” *Ecosystem Services* 52: 101362.  
592 <https://doi.org/10.1016/j.ecoser.2021.101362>.
- 593 Berzaghi, F., M. Longo, P. Ciais, S. Blake, F. Bretagnolle, S. Vieira, M. Scaranello, et al. 2019.  
594 “Carbon Stocks in Central African Forests Enhanced by Elephant Disturbance.” *Nature  
595 Geoscience* 12: 725–29. <https://doi.org/10.1038/s41561-019-0395-6>.

- 596 Berzaghi, F., R. Chami, T. Cosimano, and C. Fullencamp. 2022. "Financing conservation by  
597 valuing carbon services produced by wild animals." *Proceedings of the National*  
598 *Academy of Science USA* 119: e2120426119. <https://doi.org/10.1073/pnas.2120426119>.
- 599 Bonan, G.B. 1992. "Soil Temperature as an Ecological Factor in Boreal Forests." In *A Systems*  
600 *Analysis of the Global Boreal Forest*. Cambridge University Press.
- 601 Bradshaw C.J.A., and I.G. Warkentin. 2015. "Global Estimates of Boreal Carbon Stocks and  
602 Flux." *Global and Planetary Change* 128: 24-30.  
603 <https://doi.org/10.1016/j.gloplacha.2015.02.004>.
- 604 Brodie, J.H. 2018. "Carbon Costs and Bushmeat Benefits of Hunting in Tropical Forests."  
605 *Ecological Economics* 152: 22-6. <https://doi.org/10.1016/j.ecolecon.2018.05.028>.
- 606 Brodie, J.F., and H.K. Gibbs. 2005. "Bushmeat Hunting as Climate Threat." *Science* 326: 364-  
607 365. <https://doi.org/10.1126/science.326.364b>.
- 608 Brodie, J.F., and P.B. McIntyre. 2019. "Bushmeat Biogeochemistry: Hunting Tropical Mammals  
609 Alters Ecosystem Phosphorus Budgets." *Proceedings of the Royal Society B* 286:  
610 20190966. <https://doi.org/10.1098/rspb.2019.0966>.
- 611 Buote, P.C., B.E. Law, W.J. Ripple, and L.T. Berner. 2020. "Carbon Sequestration and  
612 Biodiversity Co-Benefits of Preserving Forests in the Western United States." *Ecological*  
613 *Applications* 30: e02039. <https://doi.org/10.1002/eap.2039>.
- 614 Busch, J., J. Engelmann, S.C. Cook-Patton, B.W. Griscom, T. Kroeger, H. Possingham et al.  
615 2019. "Potential for Low-Cost Carbon Dioxide Removal Through Tropical  
616 Reforestation." *Nature Climate Change* 9: 463-66. [https://doi.org/10.1038/s41558-019-](https://doi.org/10.1038/s41558-019-0485-x)  
617 [0485-x](https://doi.org/10.1038/s41558-019-0485-x).

- 618 CBD/WG2020/3/3. 2022. Report of the *Open-ended Working Group on the Post-202 Global*  
619 *Biodiversity Framework on its Third Meeting (Part II)*. Convention on Biological  
620 Diversity, Geneva. <https://www.cbd.int/meetings/WG2020-03>.
- 621 Chami, R., T. Cosimano, C. Fullenkamp, and D. Nieburg. 2022. "Toward a Nature-based  
622 Economy." *Frontiers in Climate* 4: 855803. <https://doi.org/10.3389/fclim.2022.855803>.
- 623 Chapin, F.S., and G. Whiteman. 1998. "Sustainable Development of the Boreal Forest:  
624 Interaction of Ecological, Social and Business Feedbacks." *Conservation Ecology* 2: 1-  
625 15. <http://www.consecol.org/vol2/iss2/art12/>
- 626 Crowther, T., K. Todd-Brown, C. Rowe, W. Wieder, J. Carey, M. Machmuller, B. Snoek, et al.  
627 2016. "Quantifying Global Soil Carbon Losses in Response to Warming." *Nature* 540:  
628 104-8. <https://doi.org/10.1038/nature20150>.
- 629 De Jager, N.R., J.J. Rohweder, B.R. Miranda, B.R. Sturtevant, T.J. Fox, and M.C. Romanski.  
630 2017. "Modelling Moose–Forest Interactions under Different Predation Scenarios at Isle  
631 Royale National Park, USA." *Ecological Applications* 27: 1317-37.  
632 <https://www.jstor.org/stable/26294490>.
- 633 Drever, C.R., C. Hutchinson, M.C. Drever, F. Fortin, C.A. Johnson, and Y.F. Wiersma. 2019.  
634 "Conservation through Co-occurrence: Woodland Caribou as a Focal Species for Boreal  
635 Biodiversity." *Biological Conservation* 232: 238-52.  
636 <https://doi.org/10.1016/j.biocon.2019.01.026>.
- 637 Enriquez, A.J., and D.C. Finnoff. 2021. "Managing mortality of multi-use megafauna." *Journal*  
638 *of Environmental Economics and Management* 107:102441.  
639 <https://doi.org/10.1016/j.jeem.2021.102441>

- 640 Fargione, J., S. Bassett, T. Boucher, S.D. Bridgham, S.C. Cook-Patton, P.W. Ellis, A. Falcucci,  
641 et al., 2018. “Natural Climate Solutions for the United States.” *Science Advances* 4:  
642 eaat1869. <https://doi.org/10.1126/sciadv.aat1869>.
- 643 Gauthier, S., P. Bernier, T. Kuuluvainen, A.Z. Shvidenko, and D.G. Schepaschenko. 2015.  
644 “Boreal Forest Health and Global Change.” *Science* 349: 819-22.  
645 <https://doi.org/10.1126/science.aaa9092>.
- 646 Girardin, C.A.J., S. Jenkins, N. Seddon, M. Allen, S.L. Lewis, C.E. Wheeler, B.W. Griscom, et  
647 al. 2021. “Nature-based Solutions Can Help Cool the Planet — If We Act Now. *Nature*  
648 593: 191-4. <https://www.nature.com/articles/d41586-021-01241-2>.
- 649 Griscom, B.W., J. Adams, P.W. Ellis, R.A. Houghton, G. Lomax, D.A. Miteva, W.H.  
650 Schlesinger, et al. 2017. “. ” *Proceedings of the National Academy of Science USA* 114:  
651 11645–50. <https://doi.org/10.1073/pnas.1710465114>.
- 652 Hebblewhite, M. 2017. “Billion Dollar Boreal Woodland Caribou and the Biodiversity Impacts  
653 of the Global Oil and Gas Industry.” *Biological Conservation* 206: 102-11.  
654 <https://doi.org/10.1016/j.biocon.2016.12.014>.
- 655 Holmberg M, T. Aalto, A. Akujärvi, A.N. Arslan, I. Bergström, K. Böttcher K, I. Lahtinen, et al.  
656 2019. “Ecosystem Services Related to Carbon Cycling – Modeling Present and Future  
657 Impacts in Boreal Forests.” *Frontiers in Plant Science* 10:343.  
658 <https://doi.org/10.3389/fpls.2019.00343>.
- 659 Houghton, R.A., and A.A. Nassikas. 2018. “Negative Emissions from Stopping Deforestation  
660 and Forest Degradation, Globally.” *Global Change Biology* 24: 350–59.  
661 <https://doi.org/10.1111/gcb.13876>.

- 662 Houghton, R. A., F. Hall, and S.J. Goetz. 2009. "Importance of Biomass in the Global Carbon  
663 Cycle." *Journal of Geophysical Research: Biogeosciences* 114, G00E03.  
664 <https://doi.org/10.1029/2009JG000935>.
- 665 Honegger, M., A. Michaelowa, and J. Roy. 2021. "Potential Implications of Carbon Dioxide  
666 Removal for Sustainable Development Goals." *Climate Policy* 21: 678–98.  
667 <https://doi.org/10.1080/14693062.2020.1843388>.
- 668 IPCC, 2022: *Climate Change 2022: Impacts, Adaptation and Vulnerability*. Contribution of  
669 Working Group II to the Sixth Assessment Report of the Intergovernmental Panel on  
670 Climate Change [H.-O. Pörtner, D.C. Roberts, M. Tignor, E.S. Poloczanska, K.  
671 Mintenbeck, A. Alegría, M. Craig, S. Langsdorf, S. Lösschke, V. Möller, A. Okem, B.  
672 Rama (eds.)]. Cambridge University Press. Cambridge University Press, Cambridge, UK  
673 and New York, NY, USA, 3056 pp. <https://www.ipcc.ch/report/ar6/wg2/>.
- 674 Jain, T.B., R.T., Graham, and D. Adams. 2010. *Carbon Concentrations and Carbon Pool  
675 Distributions in Dry, Moist, and Cold Mid-aged Forests of the Rocky Mountains*.  
676 Colorado: USDA Forest Service Proceedings RMRS-P-61.  
677 <https://www.fs.usda.gov/research/treesearch/37311>.
- 678 Jensen, W. F., R.V. Rea, C.E. Penner, J.R. Smith, E.V. Bragina, E. Razenkova, L. Balciauskas,  
679 et al. 2020. "A Review of Circumpolar Moose Populations with Emphasis on Eurasian  
680 Moose Distributions and Densities." *Alces* 56: 63–78.  
681 <https://alcesjournal.org/index.php/alces/article/view/265>.
- 682 Kielland, K., and J.P. Bryant. 1998. "Moose Herbivory in Taiga: Effects on Biogeochemistry and  
683 Vegetation Dynamics in Primary Succession." *Oikos* 82: 377–83.  
684 <https://doi.org/10.2307/3546979>.

- 685 Kooijman, E.D., S. McQuaid, M.-L. Rhodes, M.J. Collier, and F. Pilla. 2021. “Innovating with  
686 Nature: From Nature-based Solutions to Nature-based Enterprises.” *Sustainability*  
687 13:1263. <https://doi.org/10.3390/su13031263>.
- 688 Krutilla, J.V. 1967. “Conservation Reconsidered.” *The American Economic Review*, 4: 777–86.  
689 <https://www.jstor.org/stable/1815368>.
- 690 Littlefield, C.E., and A.W. D’Amato. 2022. “Identifying Trade-offs and Opportunities for Forest  
691 Carbon and Wildlife Using a Climate Adaptation Lens.” *Conservation Science and*  
692 *Practice* 4: e12631. <https://doi.org/10.1111/csp2.12631>.
- 693 Macias-Fauria, M., P. Jepson, N. Zimov, and Y. Mahli. 2020. “Pleistocene Arctic Megafaunal  
694 Ecological Engineering as a Natural Climate Solution?” *Philosophical Transactions of*  
695 *the Royal Society B* 375: 20190122. <https://doi.org/10.1098/rstb.2019.0122>.
- 696 Maher, S.M., E.P. Fenichel, O.J. Schmitz, and W.L. Adamowicz. 2020. “The Economics of  
697 ‘Conservation Debt’: A Natural Capital Approach to Revealed Valuation of Ecological  
698 Dynamics.” *Ecological Applications* 30: e02132. <https://doi.org/10.1002/eap.2132>.
- 699 McCarney, G.R., G.W. Armstrong, and W.L. Adamowicz. 2008. “Joint Production of Timber,  
700 Carbon and Wildlife Habitat in the Canadian Boreal Plains.” *Canadian Journal of Forest*  
701 *Research* 38: 1478-92. <https://doi.org/10.1139/X07-246>.
- 702 Miles, L., R. Agra, S. Sengupta, A. Vidal, and B. Dickson. 2021. *Nature-Based Solutions for*  
703 *Climate Change Mitigation*. Nairobi and Gland: (UNEP) United Nations Environment  
704 Program and (IUCN) International Union for Conservation of Nature.  
705 <https://www.unep.org/resources/report/nature-based-solutions-climate-change-mitigation>.
- 706 Mori, A.S. 2020. “Advancing Nature-based Approaches to Address the Biodiversity and Climate  
707 Emergency.” *Ecology Letters* 23: 1729-32. <http://dx.doi.org/10.1111/ele.13594>.

- 708 Natcher, D.C. 2009. "Subsistence and the Social Economy of Canada's Aboriginal North." *The*  
709 *Northern Review* 30: 83-98. <https://thenorthernreview.ca/index.php/nr/article/view/6>.
- 710 Osaka, S., R. Bellamy, and N. Castree. 2021. "Framing "Nature-based" Solutions to Climate  
711 Change." *WIREs Climate Change* 12: e729. <https://doi.org/10.1002/wcc.729>.
- 712 Osuri, A.M., J. Ratnam, V. Varma, P. Alvarez-Loayza, J. Hurtado Astaiza, M. Bradford, C.  
713 Fletcher, et al. 2016 "Contrasting Effects of Defaunation on Aboveground Carbon  
714 Storage Across the Global Tropics," *Nature Communications* 7: 11351.  
715 <https://doi.org/10.1038/ncomms11351>.
- 716 Pastor, J., B. Dewey, R. Moen, D.J. Mladenoff, M. White, and Y. Cohen 1998. "Spatial Patterns  
717 in the Moose–Forest–Soil Ecosystem on Isle Royale, Michigan, USA." *Ecological*  
718 *Applications* 8: 411-24. <https://doi.org/10.2307/2641081>.
- 719 Peres, C.A., T. Emilio, J. Schiatti, S.J.M Desmoulière, and T. Levi 2016. "Dispersal Limitation  
720 Induces Long-term Biomass Collapse in Overhunted Amazonian Forests." *Proceedings*  
721 *of the National Academy of Science U.S.A.* 113: 892-97.  
722 <https://doi.org/10.1073/pnas.1516525113>.
- 723 Petersen, T. K., A.L. Kolstad, J. Kouki, S.L. Leroux, L.R. Potvin, J.P. Tremblay, J.-P., M.  
724 Wallgren, et al. 2023. "Airborne Laser Scanning Reveals Uniform Responses of Forest  
725 Structure to Moose (*Alces alces*) Across the Boreal Forest Biome." *Journal of*  
726 *Ecology* 111: 1396–1410. <https://doi.org/10.1111/1365-2745.14093>.
- 727 Piao, S., S. Sitch, P. Ciais, P., Friedlingstein, P., Peylin, X. Wang, A. Alsröm et al. 2013.  
728 "Evaluation of Terrestrial Carbon Cycle Models for their Response to Climate Variability  
729 and to CO<sub>2</sub> Trends." *Global Change Biology* 19: 2117–32.  
730 <https://doi.org/10.1111/gcb.12187>.

- 731 Pörtner H.O., R.J. Scholes, A. Arneth, D.K.A. Barnes, M.T. Burrows, S.E. Diamond, C.M  
732 Duarte, et al. 2023. Overcoming the Coupled Climate and Biodiversity Crises and their  
733 Societal Impacts. *Science* 380: eab14881. <https://doi.org/10.1126/science.abl4881>.
- 734 Ramirez, J.I., P.A., Jansen, J. den Ouden, L. Moktan, N. Herdoiza, and L. Poorter.  
735 2021. “Above- and Below-ground Cascading Effects of Wild Ungulates in Temperate  
736 Forests.” *Ecosystems* 24 153–67. <https://edepot.wur.nl/524391>.
- 737 Rittenhouse, C.D., and A.R. Rissman. 2012. Forest Cover, Carbon Sequestration, and Wildlife  
738 Habitat: Policy Review and Modeling of Trade-offs Among Land Use Scenarios.  
739 *Environmental Science and Policy* 21, 94-105.  
740 <https://doi.org/10.1016/j.envsci.2012.04.006>.
- 741 Rizzuto, M., S.J. Leroux, and O.J. Schmitz. 2024. “Rewiring the Carbon Cycle: A Theoretical  
742 Framework for Animal-driven Ecosystem Carbon Sequestration.” *Journal of Geophysical*  
743 *Research: Biogeosciences* 129: e2024JG008026. <https://doi.org/10.1029/2024JG008026>.
- 744 Salvatori, E. and G. Pallante. 2021. Forests as Nature-based Solutions: Ecosystem Services,  
745 Multiple Benefits and Trade-offs. *Forests* 12: 800. <https://doi.org/10.3390/f12060800>.
- 746 Schmitz, O.J. 1992. “Exploitation in Model Food Chains with Mechanistic Consumer-resource  
747 Dynamics.” *Theoretical Population Biology* 41: 161-83. [https://doi.org/10.1016/0040-  
748 5809\(92\)90042-R](https://doi.org/10.1016/0040-5809(92)90042-R).
- 749 Schmitz, O.J. 2005. “Scaling from Plot Experiments to Landscapes: Studying Grasshoppers to  
750 Inform Forest Ecosystem Management.” *Oecologia* 145: 225-34.  
751 <https://doi.org/10.1007/s00442-005-0063-y>.



- 752 Schmitz, O. J. and S.J. Leroux, S. J. 2020. “Food Webs and Ecosystems: Linking Species  
753 Interactions to the Carbon Cycle.” *Annual Review of Ecology, Evolution, and*  
754 *Systematics*, 51: 271–295. <https://doi.org/10.1146/annurev-ecolsys-011720-104730>.
- 755 Schmitz, O.J., E. Post, C.E. Burns, and K.M. Johnston. 2003. “Ecosystem Responses to Global  
756 Climate Change: Moving Beyond Color-mapping.” *BioScience* 53: 1199-1205.  
757 [https://doi.org/10.1641/0006-3568\(2003\)053\[1199:ERTGCC\]2.0.CO;2](https://doi.org/10.1641/0006-3568(2003)053[1199:ERTGCC]2.0.CO;2).
- 758 Schmitz, O.J., P.A. Raymond, J.A. Estes, W.A. Kurz, G.W. Holtgrieve, M.E. Ritchie, D.E.  
759 Schindler, et al. 2014. “Animating the Carbon Cycle.” *Ecosystems* 7: 344-59.  
760 <https://doi.org/10.1007/s10021-013-9715-7>.
- 761 Schmitz, O. J., M. Sylvén, T.B. Atwood, E.S. Bakker, F. Berzaghi, J.F. Brodie, J.P.G.M.  
762 Cromsigt et al. 2023. “Trophic Rewilding Can Expand Natural Climate Solutions.”  
763 *Nature Climate Change* 13: 324-333. <https://doi.org/10.1038/s41558-023-01631-6>.
- 764 Seagle, S.W. 2003. “Can Ungulates Foraging in a Multiple-Use Landscape Alter Forest Nitrogen  
765 Budgets?” *Oikos* 103: 230–234. <https://www.jstor.org/stable/3548077>.
- 766 Seddon, N., A. Smith, P. Smith, I. Key, A. Chausson, C. Girardin, J. House et al. 2021. “Getting  
767 the Message Right on Nature-based Solutions to Climate Change.” *Global Change*  
768 *Biology* 27: 1518– 1546. <https://doi.org/10.1111/gcb.15513>.
- 769 Smith, P., A. Arneeth, D.K.A. Barnes, K. Ichii, P.A. Marquet, A. Popp, H. Pörtner et al.  
770 2022. “How Do We Best Synergize Climate Mitigation Actions to Co-benefit  
771 Biodiversity?” *Global Change Biology* 28: 2555–77. <https://doi.org/10.1111/gcb.16056>.
- 772 Sobral, M., K.M. Silvius, H. Overman, L.F.B. Oliveira, T.K. Rabb, and J.M.V. Fragoso. 2017.  
773 Mammal Diversity Influences the Carbon Cycle through Trophic Interactions in the

- 774 Amazon. *Nature Ecology and Evolution* 1: 1670-76. [https://doi.org/10.1038/s41559-017-](https://doi.org/10.1038/s41559-017-0334-0)  
775 [0334-0](https://doi.org/10.1038/s41559-017-0334-0).
- 776 Timmerman, H.R., and A.R. Rogers. 2005. "Moose: Competing and Complementary Values."  
777 *Alces* 41: 85-120. <https://alcesjournal.org/index.php/alces/article/view/413>.
- 778 Wam, H.K., O. Hofstad, E. Nævdal, and P. Sankhayan. 2005. "A Bio-Economic Model for  
779 Optimal Harvest of Timber and Moose." *Forest Ecology and Management* 206: 207–19.  
780 <https://doi.org/10.1016/j.foreco.2004.10.062>.
- 781 Watson, R.T., I.R. Noble, B. Bolin, N.H. Ravindranath, D.J. Verardo, and D.J. Dokken (Eds.),  
782 2000. *Land use, land-use change and forestry: a special report of the Intergovernmental*  
783 *Panel on Climate Change*. Cambridge University Press.
- 784 Wilmers C.C., and O.J. Schmitz. 2016. "Effects of Gray Wolf-induced Trophic Cascades on  
785 Ecosystem Carbon Cycling." *Ecosphere* 7: e01501. <https://doi.org/10.1002/ecs2.1501>.
- 786 Yona, L., B. Cashore and O.J. Schmitz. 2019. "Integrating Policy and Ecology within a Single  
787 System to Achieve Path Dependent Climate Solutions." *Environmental Science and*  
788 *Policy* 98: 54-60. <http://dx.doi.org/10.1016/j.envsci.2019.03.013>.
- 789 Zaehle, S., B.E. Medlyn, M.G. De Kauwe, A.P. Walker, M.C. Dietze, T. Hickler, T., Y. Luo et  
790 al. 2014. "Evaluation of 11 Terrestrial Carbon–nitrogen Cycle Models Against  
791 Observations from Two Temperate Free-Air CO<sub>2</sub> Enrichment Studies." *New Phytologist*  
792 202: 803–22. <https://doi.org/10.1111/nph.12697>.
- 793  
794  
795  
796

797

798

799

800

801

802

803

804

805

806

807

808

809

810

811

812

### Figure Legends

813 Fig. 1. Modeled relationships between increasing moose density and carbon stock (standing  
814 biomass of trees) and carbon loss or gain (harvested timber, and the carbon sink capacity (NEP))  
815 of a boreal forest ecosystem. The nonlinear relationship arises from an interplay between  
816 density-dependent logistic moose population growth and a saturating moose consumption rate on  
817 forest vegetation (a Type II moose functional response). The dominance of each factor varies  
818 across the moose density gradient. At low densities ( $< 0.5$  per  $\text{km}^2$ ) moose are unable to cause  
819 heavy damage to plants because their consumption of plant biomass is saturated. At high

820 densities ( $> 1.0$  per  $\text{km}^2$ ) moose are unable to increase damage to plants because of strong intra-  
821 population competition for plant biomass. The strongest moose impacts, and hence greatest  
822 change in ecosystem carbon, occurs at intermediate densities between 0.5 - 1.0 moose per  $\text{km}^2$ .

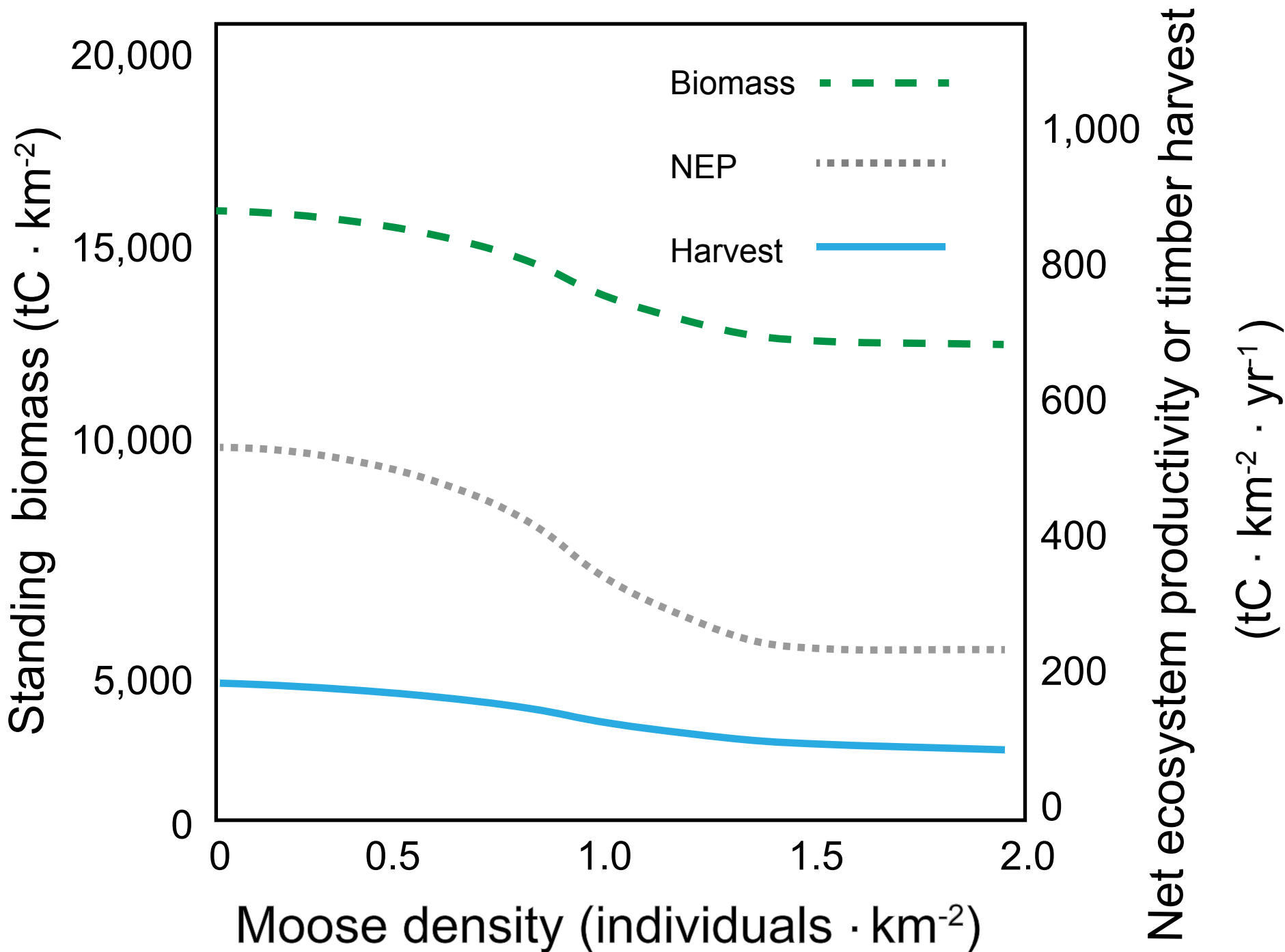
823  
824 Fig. 2. Examination of how increasing carbon prices influences the optimal density of moose in a  
825 non-harvested and harvested forest scenario to maximize the net benefits among forest  
826 harvesting, moose hunting and carbon storage. The dashed and dotted red lines and solid blue  
827 line represent different moose management scenarios. To enhance ecosystem carbon storage,  
828 moose populations could be reduced from a high density starting population (maximum  
829 sustained yield for hunting: dashed red line), reduced from a lower-density starting population  
830 (half of MSY population: dotted red line), or reduce from a low level initially set to maximize  
831 timber production (solid blue line). Regardless, maximizing net benefits from investments in the  
832 nature-based solution (ecosystem carbon storage) and timber management for harvesting  
833 incentivizes large reductions in moose population densities and hence loss in their attendant  
834 control over the forest ecosystem. That is, investments in nature-based solutions and timber  
835 encourage reducing or eliminating a key functional control of forest ecosystem dynamics, i.e.,  
836 trading-off nature for nature-based solutions.

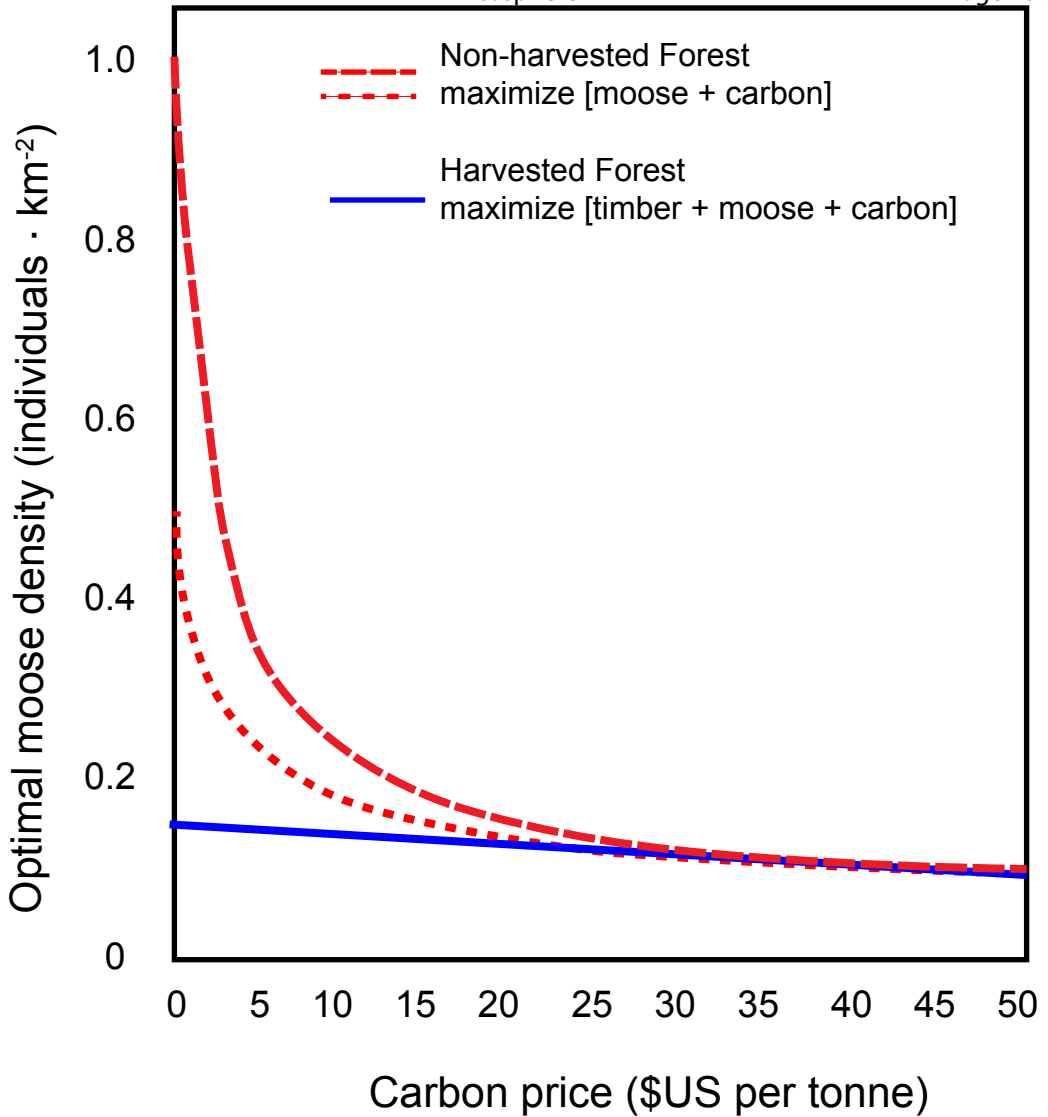
837  
838 Fig. 3. Modeled relationship between the price of carbon offsets and the amount of carbon stored  
839 in tree biomass (solid blue line) and soils (dashed red line) of a boreal ecosystem. Carbon storage  
840 in tree biomass and soil eventually saturates with increasing carbon price due to the decreasing  
841 marginal reduction in moose density ( $M$ ) as carbon price increases (Fig. 1), as well as limitations  
842 on carbon uptake imposed by natural ecological processes.

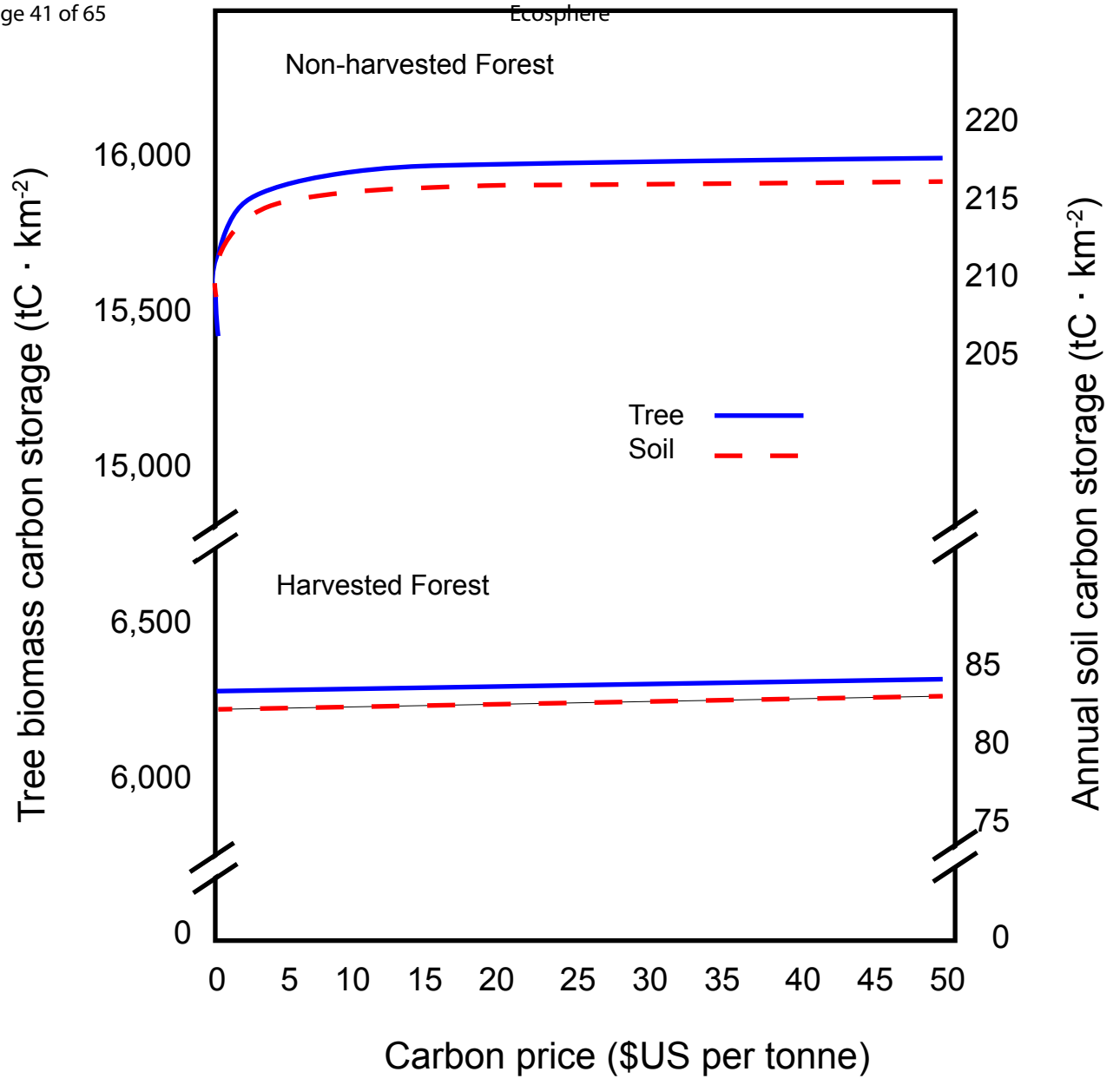
843

844 Fig. 4. The cumulative relationship between carbon price and the additional net economic benefit  
845 of investment in nature-based boreal forest carbon capture and storage. Maximizing the return on  
846 investment implies a loss of “nature” by reducing moose populations to low levels. This leads to  
847 an increasing negative return for a cultural ecosystem service—moose hunting—with increasing  
848 carbon prices.

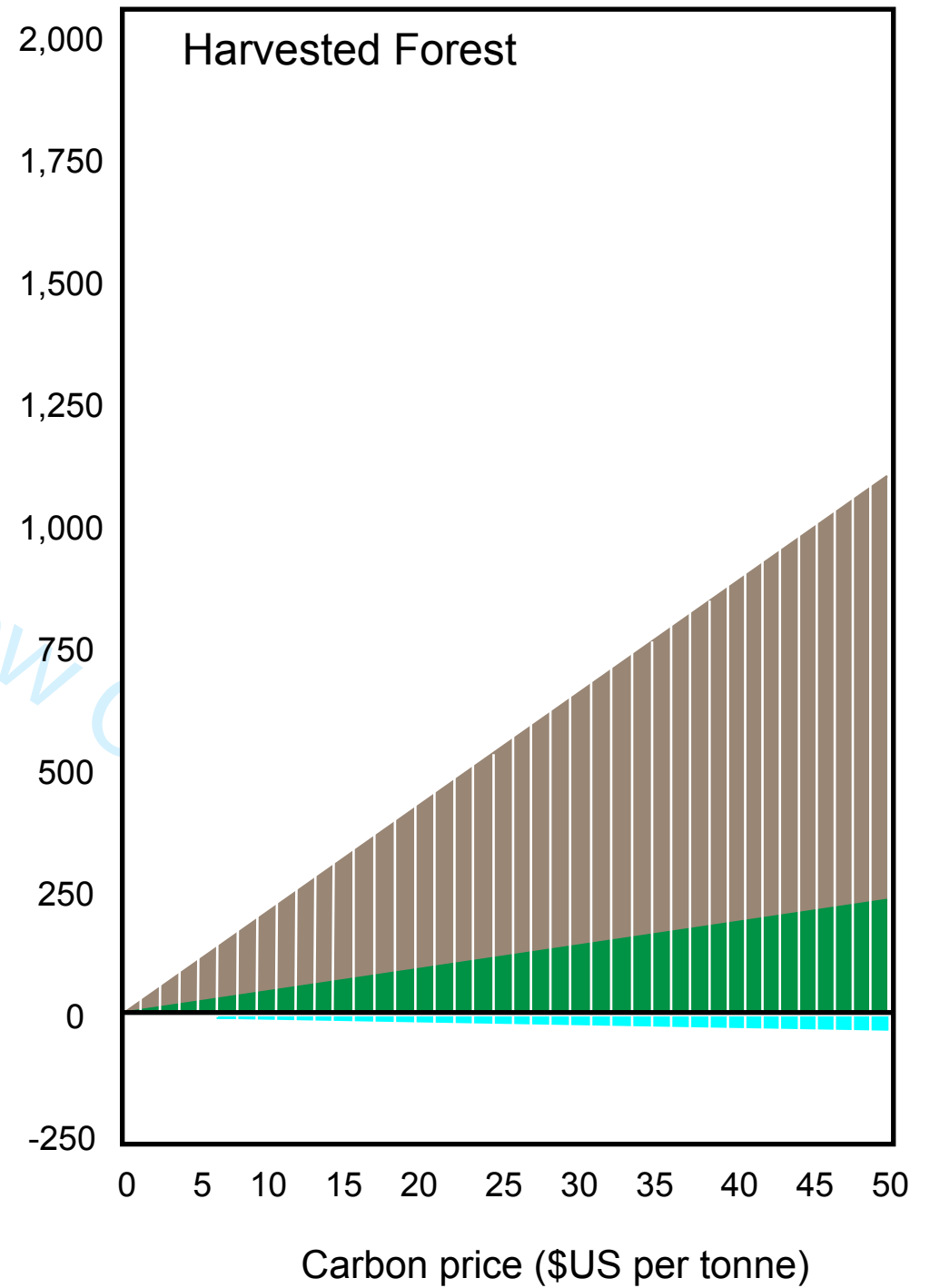
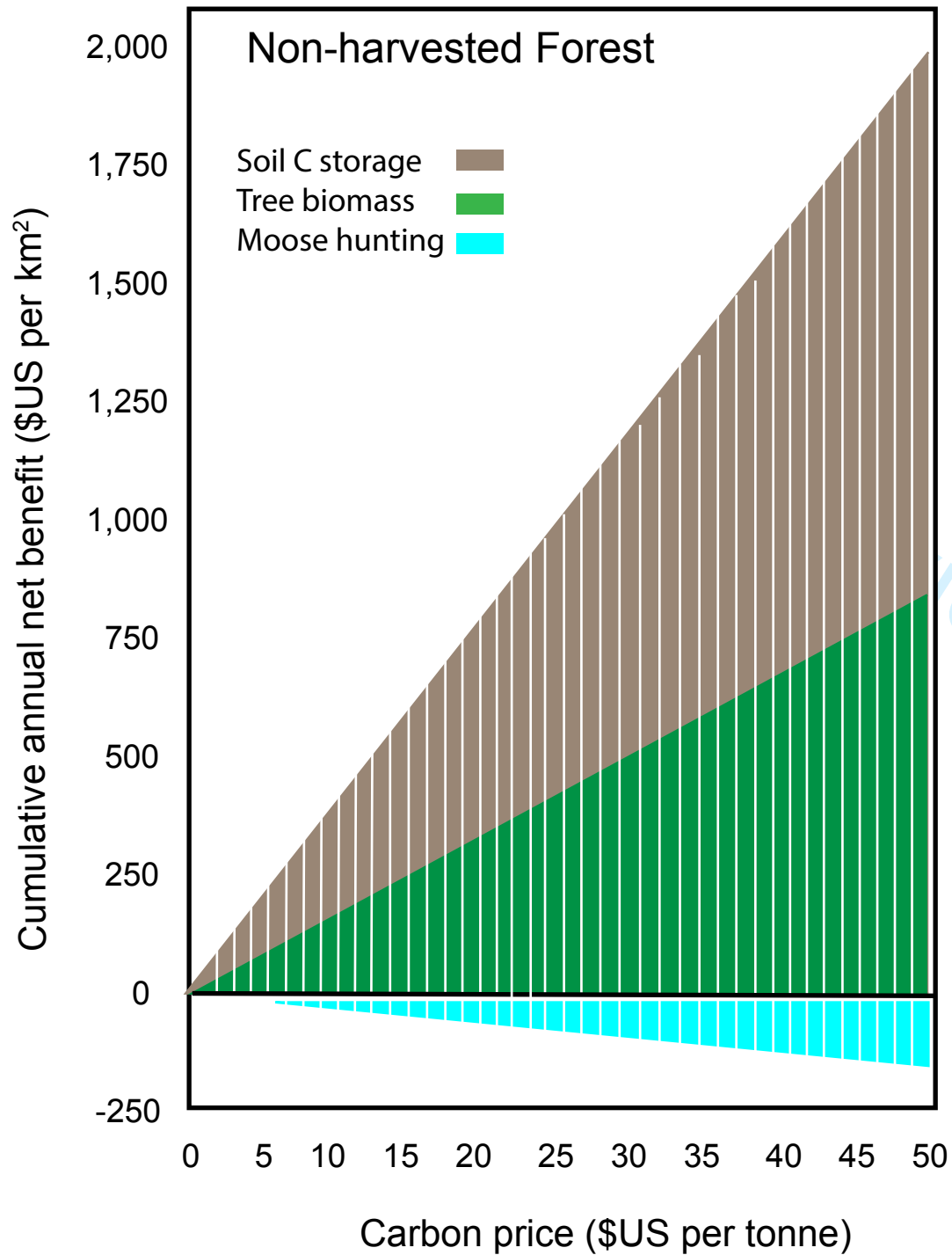
For Review Only











## APPENDIX S1

## Trading off nature for nature-based solutions: the bioeconomics of forest management for wildlife, timber and carbon

Jonah Ury, Matthew J. Kotchen, and Oswald J. Schmitz

School of the Environment, Yale University 195 Prospect Street, New Haven, CT 06511 USA

### Overview

The following narrative presents the equations and assumptions that describe the systems and system dynamics of the bioeconomic boreal forest model. The narrative further details how the models were analyzed to produce the results presented in the main text. All model parameters and functions and their literature sources are presented in Table S1. Our analysis examines the interrelationships between three main components of the bioeconomic system: the ecological system, the forest growth and yield system, and the economic system. The ecological system relates the interplay among net ecosystem productivity—aka the carbon sink potential of an ecosystem—tree biomass ( $T$ ), moose population abundance ( $M$ ), moose hunting ( $H_M$ ), forest harvesting ( $H_T$ ) and dead organic matter pools ( $OM$ ). The Forest growth and yield system characterizes merchantable timber yield ( $H_{TY}$ ), harvestable biomass, and their impacts on  $OM$ . The economic system links the two, by applying prices to  $H_M$ ,  $H_T$  and carbon storage. The following sections describe these different components of the overall model in detail.

### The Ecological Systems Model

As described in the main text, the foundational structure for this analysis is built on a dynamical systems model describing trophic interactions (Schmitz 1992) modified to explicitly link forest tree production with moose population and soil organic matter dynamics:

$$\frac{dT}{dt} = \mathcal{F}_T(T) - \mathcal{F}_M(T)M - H_T - \rho T \quad (S1)$$

$$\frac{dM}{dt} = [\varepsilon \mathcal{F}_M(T) - d_M - \Lambda M]M - H_M \quad (S2)$$

$$\frac{dOM}{dt} = \rho T + d_M M + \pi H_T - m_S OM \quad (S3)$$

where  $T$  is standing tree biomass,  $M$  is moose density,  $OM$  is the soil organic matter storage pool, and all other terms are defined as follows.  $\mathcal{F}_T(T)$  represents the net biomass growth rate of trees or net primary productivity (NPP = carbon uptake – carbon respiration) before other sources of biomass loss. These other losses include per capita moose consumption of tree biomass  $\mathcal{F}_M(T)$ , which varies functionally with tree biomass, resulting a total rate of tree biomass loss to moose that varies with moose density  $MM$ ; timber harvesting  $H_T$  at a constant rate; and loss of biomass as dead organic matter inputs to the  $OM$  storage pool at rate  $\rho T$ . Changes in moose population abundance results from consumption and assimilation of plant biomass to meet physiological needs for maintenance and reproduction  $\varepsilon \mathcal{F}_M(T)$ , where  $\varepsilon$  is the efficiency by which moose-consumed plant biomass is assimilated and converted into per capita moose growth and reproduction,  $d_M$  is the per capita natural mortality rate of moose,  $\Lambda M$  is a rate cost of density-dependent interactions among members of the moose population, and  $H_M$  is the harvest rate of moose by either natural predators or humans. We treat harvest rate of moose as a fixed control variable, given management that sets fixed levels of moose harvest by humans or sets the abundance of dominant predators (wolves) present in the ecosystem. The  $OM$  dynamics is a function of buildup due to detrital inputs from trees  $\rho T$ , death and decay of moose  $d_M M$ , debris inputs from timber harvesting  $\pi H_T$ , and loss due to soil respiration  $m_S OM$ .

Expanding on that described in the main text, we now describe the functional relationships in more detail. We assume that forest growth is bounded due to plant competition for nutrients and therefore exhibits biomass growth of the form (Schoener 1973, Tilman 1982, Schmitz 1992):

$$\mathcal{F}_T(T) = \left( \left[ \frac{RS_N}{T} \right] - m_T \right) T \quad (\text{S4})$$

where  $S_N$  is the supply rate of nutrients to the ecosystem,  $R$  is plant biomass production per unit of nutrient uptake (effectively rate of photosynthesis per unit of nutrient uptake). Accordingly,  $\frac{RS_N}{T}$  is gross production of plant biomass (GPP), and  $m_T T$  is the loss rate of plant biomass due to plant respiration, such that  $RS_N - m_T T = \text{NPP}$ .

The ability of moose to consume trees saturates with increasing tree biomass owing to physical constraints on biting and chewing imposed by the size of a moose's mouthparts (Spalinger and Hobbs 1992, Gross et al. 1993). This saturating per capita consumption rate can be described by a type-II consumer functional response:

$$\mathcal{F}_M(T) = \left[ \frac{\phi T}{1 + \beta T} \right], \quad (\text{S5})$$

where  $\phi$  represents the moose search rate for forage and  $\beta$  represents forage processing time.

This very basic characterization of forest ecosystem dynamics abstracts considerable detail found in many current carbon cycle models that explicitly account for variation in carbon content of trees due to fluxes and storage among finely divided ecosystem biomass compartments (e.g., wood, leaves, roots) and due to varying availability of soil nutrients and water. Furthermore, current carbon cycle models characterize carbon flux at explicitly physiological levels including photosynthesis (GPP), and plant and soil respiration (Piao et al. 2013, Zaehle et al. 2014). Such mechanisms can be embedded in Eqs. S1 and S3 by expressing these processes in terms of their respective rate functions (Schmitz and Leroux 2020). But expressing dynamics at this level of detail is beyond the purpose of the analysis here, which is to illustrate how to frame an economic trade-off analysis that accounts for the role of animals on carbon exchange and storage in an integrated way when reconciling competing interests. We therefore approximate this processes by assuming that any biomass accrual as  $T$  or loss of tree biomass as  $OM$  contains 50% carbon (Houghton et al. 2009, Jain et al. 2010), such that  $\alpha = 0.5$ .

### The Forest Growth and Yield Model

We examined two primary scenarios in the forest growth and yield model: the “non-harvested forest” where no timber harvest takes place (i.e.,  $H_T = 0$ ), and the “harvested forest” where some level of timber harvesting takes place (i.e.,  $H_T > 0$ ). This distinction explicitly determines the fate of plant biomass (and implicitly biomass carbon) in the ecological systems model, and hence the influence on the workings of a forest-carbon market. All equations in the forest growth and yield model delineated below operate in units of carbon mass; hence we convert the ecological biomass dynamics to biomass carbon by multiplying tree biomass by  $\alpha = 0.5$ .

Forest harvesting,  $H_T$ , results in the permanent removal of carbon from the ecosystem as merchantable timber at rate  $H_{TY}$ , and the deposition of carbon in the  $OM$  pool of the ecosystem as woody debris arising from harvesting at rate  $H_{TOM}$ . In classic forest management, timber yield is accounted in terms of volume of wood. For the purposes of carbon accounting, and for consistency with the ecological model, we assess timber harvest in terms of biomass carbon. Hence, carbon in

merchantable timber yield,  $H_{TY}$ , and in organic matter debris  $H_{TOM}$  are determined by the following equations:

$$H_{TY} = (1 - \pi) * \alpha H_T \quad (S6)$$

$$H_{TOM} = \pi * \alpha H_T = \alpha H_T - H_{TY} \quad (S7)$$

where  $H_{TY}$  represents the timber yield in tons of carbon (tC)/(time), and  $1 - \pi$  is the proportion of the timber harvest biomass  $H_T$  that is merchantable lumber, which is a function of forest age and tree composition. The  $H_{TOM}$  Eq. specifies that all non-merchantable biomass carbon is in the form of debris inputs from timber harvesting,  $\pi H_T$ , which stays in the ecosystem and is subject to decomposition.

$OM$  carbon flows in the harvested ( $h$ ) and non-harvested ( $nh$ ) scenarios follow directly from the ecological systems model:

$$OM_{nh} = \alpha \rho T - m_S OM \quad (S8)$$

$$OM_h = \alpha \rho T + H_{TOM} - m_S OM \quad (S9)$$

with litterfall rate,  $\rho$ , based on the quantity of standing biomass,  $T$ , and a per unit of  $OM$  mass decomposition rate,  $m_S$ .

### The Economic Program

The economic program is constructed to evaluate the optimal levels of moose harvesting, the key choice variable, at various carbon prices. The optimum is defined as the moose population level that maximizes the combined net benefits of timber harvesting, moose hunting, and carbon capture and storage for a range of carbon prices. Our analysis compares differences between steady-state magnitudes rather than the rate of change from one steady state to another. We define a steady state as a condition where the standing tree biomass and moose population are constant. That is, when Eqs. S1 and S2 are equal to zero, consistent with resource harvesting theory. We do not assume that Eq. S3 will equal zero, reflecting the more realistic possibility that the organic matter pool can build-up continually over time, even if management holds  $T$  and  $M$  at steady state in the forest ecosystem. For any choice of  $M$ , a steady state is defined by the functions  $\hat{T}(M)$  and  $\hat{H}_M(M)$ , which ultimately obey dynamics defined by Eqs. S1 and S2 of the ecological system.

These steady states are evaluated in terms of the net benefits of each activity to the system: moose harvesting,  $NB_{H_M}(H_M)$ , timber harvesting,  $NB_{H_T}(H_T)$ , forest carbon stored in trees,  $f$ , and forest carbon stored in organic matter,  $k$ . Net moose and timber harvesting benefits are a function of gross harvest benefits minus costs. Forest and organic matter carbon storage benefits are a function of a market for carbon sequestration where payments are based only on the additional carbon stored and a price on carbon,  $P_C$ . The following elaborates on each of these benefit pools.

### ***Moose Hunting***

We assume moose net benefits arise merely from moose hunting which can be expressed as:

$$NB_{H_M}(H_M) = B(H_M) - \kappa(H_M) \quad (S10)$$

where  $H_M$  is the steady-state hunting yield for a given managed moose population size in a given-aged forest,  $B(H_M)$  is the benefit to hunters from moose hunting, and  $\kappa(H_M)$  is the cost to moose hunters as a function of moose hunting level. To maintain a steady-state hunting yield, moose harvests  $H_M$  must equal their population growth rates implying  $\frac{dM}{dt} = 0$  with moose harvest. As such, steady-state moose yield can be described in terms of the ecological dynamical system as:

$$H_M = (\lfloor \varepsilon M(T) - d_M - \Lambda M \rfloor M)_M. \quad (S11)$$

For the purposes of calibration, we consider the objective of moose hunting in isolation of other objectives. We assume first that the objective to choose the level of moose hunting is to maximize the net benefits of moose hunting, excluding the effects on timber or other aspects of the system, such as organic matter storage and carbon. The moose benefit is evaluated using hunters' willingness to pay (WTP) as a proxy for economic benefit to hunters. For our purposes the "partial equilibrium" benefits of moose hunting can be therefore written as  $B(H_M) = WTP_M * H_M$ , where  $WTP_M$  is the willingness to pay for moose hunting at a given moose population level.

We model the costs  $\kappa(H_M)$  as an increasing and convex function, where  $\kappa'(H_M) > 0$ . We assume this cost takes the functional form  $\kappa(H_M) = \frac{\psi}{2} H_M^2$  so that the marginal cost is linear  $\kappa'(H_M) = \psi H_M$ . The net benefit (Eq. S10) is estimated as the maximized solution that satisfies  $WTP = \psi H_M$ . Rather than solve this problem, we assume this is the problem already being solved by wildlife managers, and therefore we take an estimate of  $WTP$  and an observed level of  $H_M$  to back out a calibrated value of  $\psi$ , which in turn gives us the full cost function. By linking to observed values of  $H_M$ , the cost function incorporates the manager's revealed preferences,

accounting for market and non-market values. Note that  $NB_{H_M}$  should be a concave function with a maximum value at the observed level of  $H_M$ .

### ***Timber Harvesting***

The steady state net benefits of timber harvesting are expressed as:

$$NB_{H_T}(H_T) = H_{TY}(T(M);r) * P_T - C_H(H_T) \quad (S12)$$

where  $P_T$  is the timber unit sale price,  $C_H$  is the harvest cost as a function of harvest rate, and  $r$  is the timber rotation period (therefore  $\frac{1}{r}$  is the area proportion of standing biomass harvested each year). For the purposes of this analysis—assessing tradeoffs between moose and other ecosystem services—we assume  $r$  to be a constant rotation period, resulting in a constant fraction of standing biomass harvested each year. With  $r$  constant,  $H_{TY}$  is a fully defined function of  $M$  because Eqs. S1 and S2 are assessed in steady state. As such, steady-state timber yield can be described in terms of the ecological dynamics as:

$$H_T = \mathcal{F}_T(T) - \mathcal{F}_M(T)M - \rho T \quad (S13)$$

Substituting Eqs. S13 into S12 using  $H_T$  for  $H_{TY}$  in Eq. S6 yields the complete timber harvest net benefit equation.

$$NB_{H_T}(r) = (\mathcal{F}_T(T) - \mathcal{F}_M(T)M - \rho T) * \frac{(1-\pi)*\alpha}{\lambda} * P_T - C_H(H_T) \quad (S14)$$

This equation remains a function of the fraction of biomass harvested, because  $r$  determines the level of steady-state standing biomass,  $T$ . Given moose harvesting determines the level of standing biomass as well (Eq. S1), the net benefit function also depends on moose management. Maximizing this expression with respect to the choice variable  $H_M$  tells how to manage moose when the objective is to solely maximize the net benefits of timber harvesting.

### ***Carbon Payments***

We consider a market for carbon sequestration where payments are based only on the additional carbon stored. We assume a price of carbon dioxide denoted  $P_C$ , and this is translated into a price of biomass carbon via  $\delta P_C$ . As noted previously, carbon is stored in two places relevant for our analysis: trees and soils in quantities  $\alpha T$  and  $\alpha OM$ , respectively.

Carbon payments for sequestration in trees are assumed to take the following form:

$$f = f(M;\bar{M}) = \frac{\delta P_C \alpha}{r} (\hat{T}(M) - \hat{T}(\bar{M})), \quad (S15)$$

where  $M$  is any chosen level of moose density, and  $\bar{M}$  is a corresponding baseline for comparison (see below). The carbon payments are therefore structured to compensate for the difference in standing carbon between two steady states, where the payment is expressed on an annual basis but the payment amount depends on the assumed rotation length  $r$ . This means that the forest carbon market is structured to pay for sequestration over the length of a rotation, for which we have annualized the payments.

Carbon payments for the additional increment of soil carbon were similarly structured, assuming the same  $r$  time horizon and paying only for the difference accumulated between two steady states. Before defining this payment, however, we solve for  $OM_t$  for any period  $t = 1, 2, \dots, r$  given an initial value  $OM_0$ :

$$OM_t(M; OM_0) = \rho \hat{T}(M) + d_M M + \pi \hat{H}_T(M) - m_S OM_{t-1}, \quad (\text{S16})$$

which determines the amount of loss due to decomposition during the rotation in relation to existing  $OM$  storage (note: higher levels of starting  $OM$  lead to more carbon being lost during harvesting, and more loss potential if high moose populations trigger decomposition). Given assumptions about the initial values of  $OM_0$  and a baseline steady-state equilibrium, we define the soil carbon payment as follows:

$$k = k(M; \bar{M}) = \frac{\delta P_C \alpha}{r} \sum_{t=1}^r [OM_t(M; OM_0) - OM_t(\bar{M}; \bar{OM}_0)] \quad (\text{S17})$$

The summand adds up the difference in organic matter accrual over all  $r$  periods, multiplying by  $\alpha/r$  converts the total difference into an average, annual carbon accrual, and  $\delta P_C$  translates the quantity into a payment. This average annual carbon accrual across  $r$  rotation plots means that carbon payments for soil carbon are structurally different from forest carbon payments;  $k$  represents annual average additional carbon storage between  $M$  and  $\bar{M}$ , while  $f$  utilizes  $r$  to annualize payments for the one-time change in  $T$  storage between  $M$  and  $\bar{M}$ .

**Equilibria.** Our analysis first establishes two baseline conditions to represent the equilibrium moose populations before the introduction of carbon payments for sequestration, as described further in main Manuscript (Eq. 4 and 5). The first baseline (Eq. S18) is for the non-harvested forest and maximizes the net benefits of moose hunting alone. The second baseline (Eq. S19) is for the harvested forest when moose density is chosen to maximize the net benefits to both hunters and timber harvesters.



$$M^\circ = \arg \max_M \{NB_{H_M}(\hat{H}_M(M)):H_T = 0\}. \quad (S18)$$

$$M^{\circ\circ} = \arg \max_M \{NB_{H_M}(\hat{H}_M(M)) + NB_{H_T}(\hat{H}_T(M))\}. \quad (S19)$$

Because  $\hat{H}_T(M)$  is always decreasing in  $M$ , accounting for the timber harvest in moose management will always create an incentive to lower moose density, i.e.,  $M^\circ > M^{\circ\circ}$ .

Eqs. S20 and S21 consider how the non-harvested and harvested steady state equilibria change with the introduction of a carbon payment. In particular, we consider how the conditions differ for the optimally chosen level of moose density. The level of moose density with a carbon payment in the unharvested forest case will satisfy:

$$M^* = \arg \max_M \{NB_{H_M}(\hat{H}_M(M)) + f(M;M^\circ) + k(M;M^\circ):H_T = 0\}. \quad (S20)$$

This baseline condition is used to estimate carbon payment increments relative to  $M^\circ$  in (S18). Because higher moose density leads to less standing carbon and less accumulated soil carbon, we expect  $M^* < M^\circ$ , that is, moose densities to be lower with the carbon payment. By comparing Eq. S18 to S20, we can solve explicitly for the carbon payments (for trees and soil) and the change in net benefits to moose hunters.

For a harvested forest, the choice of moose density with carbon payments will satisfy:

$$M^{**} = \max_M \{NB_{H_M}(\hat{H}_M(M)) + NB_{H_T}(\hat{H}_T(M)) + f(M;M^{\circ\circ}) + k(M;M^{\circ\circ})\}. \quad (S21)$$

The baseline condition for calibrating the payments is the solution  $M^{\circ\circ}$  in (Eq. S19). It follows that by introducing carbon payments, (Eq. S21) introduces added incentives to reduce moose density for purposes of greater benefits from timber harvesting.

Together, the moose cost and benefit equations can be used to determine the optimal moose density for the ecosystem. This optimal point occurs where the marginal moose cost equals the marginal moose benefit, where  $MC_m$  and  $MB_m$  are the marginal cost and marginal benefit, respectively:

$$MC_m = MB_m \quad (S22)$$

$$\frac{dC_m}{dt} = \frac{dB_m}{dt}$$

$$\frac{d(FB_{M=x} - FB_{M=0})}{dt} = \frac{d(WTP_{M=x})}{dt}$$

### Bioeconomic Analysis

Deriving analytical solutions for the bioeconomic system is challenging given the number of equations involved and their inherent nonlinearities. For the purposes of this study, we instead opted to conduct the analyses numerically. Our approach involves examining carbon dynamics across gradients of moose population density as managed through moose hunting. Like our Economic Program, the numerical analysis thus examines carbon dynamics in terms of steady-state conditions for Eqs. S1, S2, and S3. These steady states permit expressing each of the variables ( $T$ ,  $M$  and  $OM$ ) as functions of the other variables and moose and timber harvesting levels to conduct a carbon accounting of the boreal ecosystem, within a set of bounded conditions.

### Empirical relationships

We derive the empirical relation between net ecosystem productivity (NEP) and moose population density based on measurements from moose enclosure experiments (McInnes et al. 1992). These experiments suggest that boreal NEP without moose present results in 421 tC uptake km<sup>-2</sup> year<sup>-1</sup>, declining to 401.7 tC km<sup>-2</sup> year<sup>-1</sup> at low moose density and declining further to 319.5 tC km<sup>-2</sup> year<sup>-1</sup> at high moose density (Schmitz et al. 2014). Here we define low moose densities as 0.5 moose per km<sup>2</sup> and high moose densities as 1–1.5 moose per km<sup>2</sup> (Schmitz et al. 2014). We use a nonlinear moose-carbon relationship given moose's type-II functional response and the nonlinear effects of moose density on timber damages (Wam et al. 2005). Hence, NEP varies with moose density in an inverse sigmoidal manner (Table 1) where the marginal impact of increasing moose density is most significant between 0.3 and 1.25 moose per km<sup>2</sup>. We generated an empirical sigmoid curve using a cubic spline regression fit through the above estimates of carbon uptake in relation to moose density (Main text Fig. 1).

This NEP-moose population relationship dictates the carbon dynamics for moose impacts on the forest ecosystem. We assume that varying moose impacts on carbon storage change only in direct proportion to standing tree biomass (as opposed to further altering carbon uptake by altering photosynthetic rates). This assumption is corroborated by a simulation of moose impacts on standing biomass showing that the steady-state impacts of moose foraging at low and high

population densities decrease standing biomass carbon by approximately 25% (De Jager et al. 2017), in line with our estimate above of carbon impact in relation to moose density calculated from the independent experimental data. Therefore, moose impacts on NEP are used as a measure of moose impacts on standing biomass, while carbon impacts from timber harvesting are governed by the mass and growth of standing biomass itself.

The second empirical relationship concerns the maximal range of natural moose densities to be considered in the moose hunting analysis and its feedback on NEP. Moose hunting yields can be calculated using the traditional sustainable yield (MSY) curve, obtained by taking the derivative of the moose logistic growth function with respect to population density (Eq. S2), but excluding moose harvest ( $H_M$ ). This curve peaks at half of the carrying capacity, where carrying capacity is defined as  $K_M = \frac{\varepsilon \mathcal{F}_M(T) - d_M}{\Lambda}$  (from Eq. S2, assuming no hunting) with a MSY of  $\frac{K_M r_M}{4}$  (Getz 2012; Clark 2010). We assume a moose carrying capacity of 2.0 per km<sup>2</sup> based on a region of boreal forest absent from hunting or predation (Crête 1989). Intrinsic growth rates ( $r_M = \varepsilon \mathcal{F}_M(T) - d_M$ ) in Eq. S2 of moose is estimated to be 0.4 (Solberg et al. 2003; Wam et al. 2005). Assuming that this intrinsic population growth rate value reflects saturated consumption rates of tree biomass by moose (i.e.  $\mathcal{F}_M(T) = \max$ ), we apply this rate and carrying capacity to yield a maximum sustained hunting rate of 0.2 moose per km<sup>2</sup> per year (Table S1). Since moose harvest yields must be zero when moose are absent or at their carrying capacity,  $K_M$  ( $K_M$  implies no hunting pressure), these assumptions bound a sustained yield curve for different moose harvest levels,  $H_M$ .

Forest age can impact moose populations as well, with very young or old forests offering levels of forage quantity and quality that decreases moose carrying capacity. Fully mature forests offer less nutritious biomass, much of which is above the browsing height of moose. While young forests (such as those immediately post-timber harvest) exhibit highly nutritious forage opportunities, they lack the total biomass to support a high moose population. Only in boreal forests of intermediate ages do conifers such as spruce and pine offer ample and highly nutritional forage at browsing height (Hjeljord, et al. 1990; Randveer and Heikkilä 1996; Jiang et al. 2005) leading to carrying capacities higher than 2.0 moose per km<sup>2</sup>. For the purposes of simplifying our analysis, meant to illustrate the process, we assume that a carrying capacity of 2.0 moose per km<sup>2</sup> applies across both non-harvested and harvested forests (Hjeljord et al. 1990).

### Moose abundance, timber yield and forest carbon

We consider carbon dynamics and forest harvest yields across a range of moose densities. This analysis considers the steady-state carbon flows and harvest yields between the empirical boundary conditions: moose absence to moose carrying capacity (2 moose per km<sup>2</sup>). We translate the effect of a varying NEP-moose density relationship on timber biomass and growth by applying a timber and biomass loss factor derived from the moose-NEP relationship described above. Using the TIPSY forest biomass simulator and Chapman Richards functions employed by Asante et al. (2011) as a starting point (moose absence), we apply a percentage reduction to biomass and timber yield proportional to our documented moose-NEP reductions. This assumes that moose impact on standing biomass varies in proportion to their impact on NEP, which is supported by simulation analyses (De Jager et al. 2017). The parallel impact of moose browsing on NEP and on standing biomass and timber yields across the range of moose population densities is illustrated in Fig 1 (main text).

We illustrate the steps that are taken to arrive at a solution for the bioeconomic model, by applying representative values for the dynamical system presented above. We present solutions assuming that the dynamical system is at a steady state in our numerical analysis, thereby facilitating analyses of change in discrete increments of time and in ways that align our dynamical ecosystems model with forest harvest management modeling.

To do so, we integrate forest biomass,  $T$ , timber yield,  $H_{TY}$ , and the  $OM$  dynamics into the carbon-forestry model of Asante et al. (2011). We estimate  $T$  and  $H_{TY}$  for any forest age  $t = 1, 2, \dots, n$ , by estimating the standing timber biomass and standing timber yield,  $T_t$  and  $V_t$  respectively, adapted from the Chapman-Richards functions in Assante et al. (2011):

$$T_t = T = b_1(1 - e^{-b_2 t})^{b_3} \quad (\text{S23})$$

$$V_t = \frac{V_1(1 - e^{-V_2 t})^{V_3}}{\lambda} \quad (\text{S24})$$

$$H_T = \frac{T}{\tau r} = \frac{T_{t=r}}{r} \quad (\text{S25})$$

$$H_{TY} = (1 - \pi)H_T = \frac{V_{t=r}}{r} \quad (\text{S26})$$

Whereas  $H_{TY}$  and  $H_T$  represent the harvest rates per unit time,  $T_t$  and  $V_t$  are the total biomass and harvest yield for a certain forest area. These discrete-time estimates translate to harvest rates by

dividing the standing biomass level by the rotation period  $r$ , and  $\tau$  which is the proportion of overall biomass held in the oldest stand age ( $T_r V_r$ ). Therefore,  $\tau$  translates the rotation period into a biomass fraction of the total forest area.

For standing timber yield ( $V_t$ ), we convert the volumetric yield accounting of Asante et al. (2011) to mass of merchantable timber carbon, to make yield compatible with the biomass carbon dynamics represented in the ecological system.  $\lambda$  converts timber volume ( $\text{m}^3/\text{km}^2$ ) into tons of merchantable timber carbon ( $\text{tC}/\text{km}^2$ ). For the purposes of this analysis, we assign  $\lambda$  a constant value of  $0.2$  ( $\text{tC}/\text{m}^3$ ) to reflect an estimated carbon content of  $200$  kg per  $\text{m}^3$  of wood (Jessome 1977).

In these equations  $b_x$  and  $v_x$  are regression parameters that determine the slope and shape of the forest and merchantable timber growth curves. Based on the TIPSYS forest biomass simulator modelled by Asante et al (2011), parameters  $b_1$ ,  $b_2$ , and  $b_3$  have been determined to be  $19,860$ ,  $0.0253$ , and  $2.64$ , respectively. Similarly, parameters  $v_1$ ,  $v_2$ , and  $v_3$  are determined to be  $50,040$ ,  $0.027$  and  $4.003$ , respectively (Asante et al. 2011). These two growth equations replace the need to estimate the proportion of biomass that is merchantable,  $(1 - \pi)$ , estimated instead with the equation  $H_{TOM} = T_t - V_t$ . To vary Eqs. S23 and S24 for the impact of moose browsing, we apply the timber and biomass loss factors outlined above.

Organic matter inputs in a given time period  $OM_t$  represents the total  $OM$  in year  $t$  coming from natural litterfall and debris inputs from timber harvesting.  $OM$  inputs are examined in discrete time using equations that are annualized adaptations of the Forest Growth and Yield Model linked to the discretized dynamical ecosystems model where

$$OM_{nht} = (1 - m_S)OM_{nht-1} + \rho T_t \quad (\text{S27})$$

$$OM_{ht} = (1 - m_S)OM_{ht-1} + \rho T_t + H_{TOM}. \quad (\text{S28})$$

This set of equations accounts for  $OM$  in year  $t$  in relation to all  $OM$  from the previous year not lost to soil respiration, plus the addition of any litterfall,  $\rho T_t$ , or harvest inputs  $H_{TOM}$ .

The forest carbon market considers the annual change in soil carbon, tree biomass, and merchantable timber volume. The annualized equations facilitate calculating the annual change in total ecosystem carbon to determine the annual carbon payment or liability. The average of all

$OM_t$  from  $t = 0$  to  $t = r$  represents the average of all forest plots. In turn, this average results in the net annual OM accrual or loss from the system across the entire forest plot.

We assume that old growth forests have an average stand age of 100 years (McCarthy and Weetman 2006, McLaren and Peterson 1994). In line with common boreal forestry practices, our model assumes that managed forests are spruce and pine stands managed as even-aged stands. For boreal stands without a forest carbon market,  $\sim 80$  years tends to be the ideal age to clear-cut a forest stand. In turn, a rotation of  $1/80^{\text{th}}$  size plots harvested annually ensures consistent revenues (Asante et al. 2011). In the numerical analysis we assume that harvested forest stands revert to a stand age of 0, with all non-harvested biomass remaining in the system as dead organic matter as outlined above. Upon harvest, we assume all non-merchantable biomass, such as roots, bark and branches, enters the  $OM$  pool, and all harvested timber is removed from the ecosystem. Because the carbon market considers *changes* in ecosystem carbon, it treats harvested biomass as an emission (Asante et al. 2011; United Nations Environment Programme 2009). The  $OM$  pool increases due to litterfall and harvest additions and decreases due to the decomposition of biomass to  $CO_2$ .

Values for decomposition rate,  $m_S = 0.00841$ , and litterfall rate,  $\rho = 0.01357$ , used in our analysis come from the same TIPSYS simulation designed for forest plantations (Asante et al. 2011). While litterfall rates likely remain the same, the dense forest cover and cool soil of mature forests inhibits decomposition in old growth forests. Because significant decomposition in old growth forests can occur under heavy browsing which may open up the forest canopy, we apply the decomposition rate,  $m_S$ , to the non-harvested forest scenario only when moose populations exceed 0.8 moose per  $km^2$ , the threshold designated for high moose-carbon impacts. To smooth the transition between no decomposition and full decomposition, we assume an incremental increase in decomposition rate from  $0.1m_S$  at 0.55 moose per  $km^2$  to  $m_S$  for moose densities above 0.8 per  $km^2$  (Bonan 1992; Kielland and Bryant 1998; Schmitz et al. 2003).

## Numerical Analyses

Our bioeconomic analysis involves converting the economic and ecological program into empirical benefit functions. To this end, we have financially quantified the steady-state harvest yields and carbon flows in relation to moose abundances to consider trade-offs among competing

actors on the same landscape. Here, the numerical analysis estimates the optimal levels of moose and timber harvesting at various carbon prices by quantifying the net financial implications of the competing interests according to the maximands in Eqs. S18 through S21.

### ***Moose Benefit***

Moose harvest benefits equate to the number of moose harvested annually multiplied by the benefit of each successful moose harvest, as shown in Eq. S13. Both the level of harvesting and the benefit per harvest are a function of the moose population density. Our moose harvest assumptions reflect the trend depicted in Fig. 2 of the main text, based on a simplified solution to the steady-state dynamical system. As this only considers the benefits to moose hunters (Eq. S13), we use hunter's willingness to pay (WTP) per moose to quantify moose harvest benefits. [Notably, there are other moose benefits not considered here that can be incorporated into bioeconomic models using this same methodology \(e.g., sighting value, non-use value\).](#)

A recent survey of hunters in Sweden examined WTP under three different moose populations (Mattsson et al. 2014). These values represent WTP to participate in a year's hunt, excluding additional costs for equipment and travel. It therefore reflects the net benefit value for the moose hunt itself, a suitable proxy for hunters' benefits. Adjusting for historical local inflation and expressing WTP as 2021 US dollars values yields WTP values of \$692, \$844, and \$964 for equivalent densities of 0.5 1.0 and 2.0 moose per km<sup>2</sup>, respectively (Lavsund, Nygrén, and Solberg 2003).

Following standard practice, we express the relationship between WTP and moose density as a logarithmic function. To produce a financial yield curve, we multiply WTP per moose by the sustainable harvest per year for a given moose density where moose density is determined by the level of forest harvesting. This annual hunting benefit represents the annual steady-state revenue curve for a forest with a maximum carrying capacity of 2.0 moose per km<sup>2</sup>.

### ***Forest Harvest Benefits***

Harvest benefits are estimated using a simple estimation of timber harvest profits. To financially quantify Eq. S14, we construct a basic forestry cost and revenue function applicable to a range of standing biomass levels, representative of the range of moose densities. This leverages the harvest expenses and timber sale price estimates from the same carbon-forestry model that produced the

Chapman Richard's functions (Asante et al. 2011). Converted to present US dollars, the model assumes that every ton of merchantable biomass processed costs \$199.9 to harvest and generates \$375.9 of revenue. These expenses include hauling, milling, and overhead costs. Additionally, every square kilometer of forest costs \$525,625 for road construction and harvesting, and \$105,125 for replanting after harvest (Asante et al. 2011). Based on Eq. S25, each square kilometer of 80-year old forest contains just over 6,100 tons of merchantable biomass carbon (30,000 cubic meters), worth an estimated 2.3 million dollars in revenue and \$450,000 in profit, depending on timber prices. These cost and revenue assumptions serve as the starting point from which we differentiate moose impacts on forestry yields. Applying our moose and biomass loss factors to the estimated timber yield in Eq. S25, we create a moose population-specific forest profit function. In turn, we can estimate the change in timber harvest benefits across the range of moose densities, the harvest curve depicted in Fig. 1 in the main manuscript.

### ***Carbon Payments***

We numerically estimate carbon payments across the range of moose densities by applying the empirical assumptions to moose, forest, and timber dynamics into Eqs. S16 and S17.  $\hat{T}(M)$  is estimated using the Chapman Richards function for biomass by stand age (Eq. S23) and the moose-carbon inverse sigmoidal loss factor.

The change in soil carbon payments (Eq. S17) are estimated by applying the empirical assumptions to Eqs. S27 and S28. Although soil carbon storage varies spatially, we assume the 34,000 tC per km<sup>2</sup> average to be standard across the boreal (Watson et al. 2000). After harvest, forest stands approximately aged 0-25 years see net carbon loss due to the decomposition of the  $H_{TOM}$  outweighing forest regrowth. Between stand ages of 20 and 30 years, we assume that  $OM$  decomposition progressively diminishes to zero in year 30, unless moose over-browsing or further harvest occurs. This assumption is driven by the acceleration of biomass regrowth and forest canopy cover, and the system's return to its initial  $OM$  conditions. This culminates in an assumption of net carbon loss for stands age 0 to approximately 25 years, and net carbon accrual and therefore positive carbon payments begin thereafter. As described in Eq. S17, the net change in  $OM$  additions are estimated by taking the average of all  $r$  forest plots, here estimated as the average annual  $OM$  delta from Eqs. S27 and S28. We have chosen to exclude  $d_M M$  as carbon



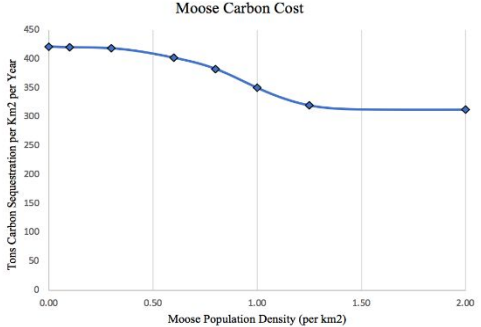
inputs from moose mortality, as they are assumed to be negligible relative to the other carbon drivers assessed here.

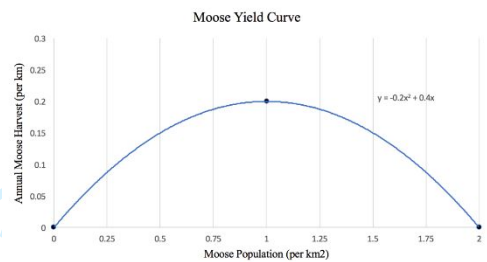
### ***Equilibria***

With each benefit function numerically estimated, the equilibria moose population at a given carbon price is the maximum of the combined total benefits across each benefit function. This solution is the maximum of Eqs. S20 and S21 according to the baseline moose populations before (Eq. S18) and after the introduction of timber harvesting (Eq. S19). Our baseline starting moose population has been estimated for both  $M^* = 0.5$  and  $M^* = 1.0$  in Eq. S18. The results of these maximand solutions are shown in Fig. 3 and Fig. 4, in the main text.

Table S1. Description of parameters used in the modeling, their values and the source for the estimates.

Parameter	Description	Numerical Model	Notes	Citation
T	Standing tree biomass	Estimated using Chapman Richards Function (Eq. S22) for biomass by forest stand age. From this, moose and harvest losses are subtracted accordingly	In the non-harvested forest case, T is estimated assuming average stand age of 100 years in (Eq. S22). In the harvested case, total T is the average of all rotation plots ages 0 to r	TIPSY forest biomass simulator; Asante et al (2011)
$\mathcal{F}_T(T)$	Net biomass growth rate of trees or net primary productivity  (NPP = carbon uptake – carbon respiration) before other sources of biomass loss.	Estimated by comparing discrete-time annual intervals in Chapman Richards Function (Eq. S22)	Growth is numerically determined by taking $(T_t - T_{t-1})$ , or can be solved by taking the derivative of $T_t$ .	TIPSY forest biomass simulator; Asante et al (2011)
M	Moose Density	Choice variable, determined by $H_M$	Assessed in this report from zero to carrying capacity, $K_M$	
$\alpha$	Fraction of Biomass that is carbon	Assumed as a constant fraction 0.5 of T and OM of biomass		(Houghton et al. 2009, Jain et al. 2010)
$H_T$	Timber harvest rate	Steady-state harvest rate is calculated based on the forest rotation time, r, where the annual harvest is the oldest 1/80 <sup>th</sup> of the forest plot, with biomass levels equal to forest age r (Eq. S24).	The impact of carbon pricing on the optimal rotation period has not been assessed in this analysis, though the addition of carbon and moose cost/benefits may motivate changes to this rotation depending on the economic program.	Asante et al (2011)
r	The timber rotation period	assumed at a fixed 80-year rotation $\frac{1}{r}$ is the areal proportion of standing biomass harvested each year		
$\tau$	The proportion of overall biomass held in the oldest stand age of the forest rotation	Used to convert rotational period into biomass fraction to estimate $H_T$ . Using the chapman Richards functions, timber yields can be		

		calculated using (Eq. S23), avoiding the need to explicitly estimate $\tau$ .		
$H_{TY}$	Merchantable timber yield	Estimated using Chapman Richards Function (Eq. S23) for harvest yield by forest stand age.	Can be used to estimate either biomass or timber volume yield with coefficient $\lambda$	TIPSY forest biomass simulator; Asante et al (2011)
$\lambda$	Coefficient of timber volume ( $m^3$ ) per tons of merchantable timber carbon	we assign $\lambda$ a constant value of 0.2 to reflect an estimated carbon content of 200 kg per $m^3$ of wood		(Jessome 1977)
$\mathcal{F}_M(T)M$	Moose consumption of tree biomass	For moose-biomass losses, we converted the NEP-moose relationship into a 1:1 biomass-loss factor. We use a nonlinear moose-carbon relationship given moose's type-II functional response and the nonlinear effects of moose density on timber damages.	The graph below shows the inverse sigmoidal relationship between forest carbon/timber and moose density in our assumptions. 	(McInnes et al. 1992) (Schmitz et al. 2014) (Wam et al. 2005) (De Jager et al. 2017)
$[\varepsilon\mathcal{F}_M(T) - d_M - \Lambda M]M$	The moose growth function excluding hunting, specifically:  $\varepsilon$ is the efficiency by which moose-consumed plant biomass is assimilated and converted into per capita moose growth,	The moose population growth curve is estimated using a logistic growth function with respect to population density	We assume a moose carrying capacity, $K_M$ , of 2.0 per $km^2$ based on a region of old growth boreal forest absent from hunting or predation. Intrinsic growth rates ( $r_M = \varepsilon\mathcal{F}_M(T) - d_M$ ) of moose is estimated to be 0.4 from a study in Scandinavia.	(Crête 1989) (Solberg et al. 2003; Wam et al. 2005)

	<p><math>d_M</math> is the per capita natural mortality rate of moose,  <math>\Lambda M</math> is a rate cost of density-dependent interactions among members of the moose population</p>			
<p><math>H_M</math></p>	<p>Sustained harvest rate of moose</p>	<p>Moose hunting yields for any are calculated using a traditional sustainable yield curve, the derivative of the logistic growth function above.</p>	<p>Sustained hunting yields are increasing up to <math>\frac{1}{2}K_M</math>, here assumed to be 1 moose per km<sup>2</sup>.</p> 	<p>(Getz 2012; Clark 2010)</p>
<p><math>WTP_M</math></p>	<p>Hunters' willingness to pay for moose hunting (per moose) at a given moose population level</p>	<p>WTP is assumed at \$692, \$844, and \$964 per moose for equivalent densities of 0.5 1.0 and 2.0 moose per km<sup>2</sup></p>	<p>Moose benefit is evaluated using hunters' willingness to pay (WTP) as a proxy for economic benefit to hunters. This is multiplied by <math>H_M</math> to calculate total moose benefits (Eqs. S10 and S11).</p>	<p>(Lavsund, Nygrén, and Solberg 2003)  <a href="#">(Mattsson et al. 2014)</a></p>
<p><math>d_M M</math></p>	<p>debris inputs from the natural mortality rate of moose</p>	<p>Carbon from dead moose is considered negligible (for OM) so excluded from the model.</p>	<p>Mortality is naturally incorporated into the sustained yield curve for steady-state moose populations.</p>	

$\pi H_T$	Debris inputs from timber harvesting, where $\pi$ is the proportion of harvested biomass that is not sold	Non-merchantable biomass is estimated using Chapman Richards Function (Eqs. S23 and S24), where $\pi H_T = T_t - V_t$ .	All non-merchantable biomass is assumed to be left in-situ in the OM pool.	TIPSY forest biomass simulator; Asante et al (2011)
$\rho T$	The rate of natural detrital inputs from standing biomass	Litterfall rate is taken as a constant of standing biomass, where $\rho = 0.01357$		TIPSY forest biomass simulator; Asante et al (2011)
$m_S$	The soil respiration rate of OM	Similar to litterfall, decomposition rate is taken as a constant of OM biomass for managed timber rotations, where $m_S = 0.00841$ . In mature forests with sufficient canopy cover for cool soils, decomposition may be near-zero. To account for this, no decomposition is included ( $m_S = 0$ ) for forest plots over 30 years old, scaled down progressively starting in stand age 20.	Similarly, heavy moose browsing can open up the forest canopy, triggering decomposition non-harvested mature forests. We apply the decomposition rate, $m_S$ , to the non-harvested forest scenario when moose populations exceed 0.8 moose per km <sup>2</sup> , the threshold designated for high moose-carbon impacts. We assume an incremental increase in decomposition rate from $0.1m_S$ at 0.55 moose per km <sup>2</sup> to $m_S$ for moose densities above 0.8 per km <sup>2</sup>	(Bonan 1992; Kielland and Bryant 1998; Schmitz et al. 2003)
$P_C$	Carbon Price	Varied from \$0 to \$50 <u>per ton of CO<sub>2</sub></u> across the analysis		
$\delta$	Mass conversion of carbon dioxide to carbon	To convert a carbon dioxide price into a biomass carbon price	A constant 3.67	

<p><math>OM</math></p>	<p>Organic matter, where <math>OM_0</math> represents the existing OM in the system before adjustments in moose management.</p>	<p><math>OM_0</math> is assumed at 34,000 tC per km<sup>2</sup> for all cases.</p> <p>The model simplifies the dynamical OM system by using annual discrete-time equations (Eqs. S25 and S26) in line with the annual Chapman Richards forest equations.</p>	<p>Like T, the average annual <math>dOM</math> is calculated as the average of all <math>r</math> forest rotation plots to determine the steady-state level of OM accrual or decomposition.</p> <p>The steady state condition for <math>\frac{dOM}{dt}</math> (Eq. S3) is assumed to be constant, though unlike <math>\frac{dT}{dt}</math> (Eq. S1), <math>\frac{dOM}{dt} \neq 0</math>.</p>	<p>(Asante et al. 2011; United Nations Environment Programme. 2009; Schmitz et al. 2003, Watson et al. 2000)</p>
<p><math>P_T</math></p>	<p>The timber unit sale price</p>	<p>Assumed to be \$375 per ton</p>	<p>Often described as a function of volume rather than mass. Multiplying by <math>\lambda</math> yields sale price \$75 per m<sup>3</sup>.</p>	<p>(Asante et al. 2011)</p>
<p><math>C_H(H_T)</math></p>	<p>The harvest cost as a function of harvest rate</p>	<p>\$200 per ton for hauling, milling, and overhead costs. Plus fixed costs per km<sup>2</sup> of \$525,625 for road construction and harvesting, and \$105,125 for replanting after harvest</p>	<p>\$200 per ton equates to \$40 per m<sup>3</sup> using coefficient <math>\lambda</math>.</p>	<p>(Asante et al. 2011)</p>

## References

- Asante, P., G.W. Armstrong, and W.L. Adamowicz. 2011. "Carbon Sequestration and the Optimal Forest Harvest Decision: A Dynamic Programming Approach Considering Biomass and Dead Organic Matter." *Journal of Forest Economics* 17: 3–17.
- Bonan, G.B. 1992. "Soil Temperature as an Ecological Factor in Boreal Forests." In *A Systems Analysis of the Global Boreal Forest*. Cambridge University Press.
- Clark, C.W. 2010. *Mathematical Bioeconomics: The Mathematics of Conservation*. John Wiley & Sons.
- Crête, M. 1989. "Approximation of K Carrying Capacity for Moose in Eastern Quebec." *Canadian Journal of Zoology* 67: 373–80.
- De Jager, N.R., J.J. Rohweder, B.R. Miranda, B.R. Sturtevant, T.J. Fox, and M.C. Romanski. 2017. "Modelling Moose–Forest Interactions under Different Predation Scenarios at Isle Royale National Park, USA." *Ecological Applications* 27: 1317–37.
- Getz, W. 2012. "Harvesting Theory." *Encyclopedia of Theoretical Ecology* 4:346.
- Gross, J.E., L.A. Shipley, N.T. Hobbs, D.E. Spalinger and B.A. Wunder. 1993. "Functional Response of Herbivores in Food-concentrated Patches: Test of a Mechanistic Model." *Ecology* 74:778-91.
- Hjeljord, O., N. Hövik, and H.B. Pedersen. 1990. "Choice of Feeding Sites by Moose during Summer, the Influence of Forest Structure and Plant Phenology." *Holarctic Ecology* 13: 281–92.
- Houghton, R.A., and A.A. Nassikas. 2018. "Negative Emissions from Stopping Deforestation and Forest Degradation, Globally." *Global Change Biology* 24: 350–59.
- Houghton, R. A., F. Hal, and S.J. Goetz. 2009. "Importance of Biomass in the Global Carbon Cycle, *Journal of Geophysical Research* 114, G00E03
- Jain, T.B., R.T., Graham, and D. Adams. 2010. *Carbon Concentrations and Carbon Pool Distributions in Dry, Moist, and Cold Mid-aged Forests of the Rocky Mountains*. Colorado: USDA Forest Service Proceedings RMRS-P-61.
- Jessome, A. P. 1977. "Strength and Related Properties of Woods Grown in Canada." *Forestry Technical Report Eastern Forest Products Laboratory (Canada). No. 21*.
- Jiang, Z., H. Ueda, M. Kitahara, and H. Imaki. 2005. "Bark Stripping by Sika Deer on Veitch Fir Related to Stand Age, Bark Nutrition, and Season in Northern Mount Fuji District, Central Japan." *Journal of Forest Research* 10: 359–65.

- Kielland, K., and J.P. Bryant. 1998. "Moose Herbivory in Taiga: Effects on Biogeochemistry and Vegetation Dynamics in Primary Succession." *Oikos* 82: 377–83.
- Lavsund, S., T. Nygrén, and E.J. Solberg. 2003. "Status of Moose Populations and Challenges to Moose Management in Fennoscandia." *ALCES* 39: 109-30.
- Mattsson, L., M. Boman, and E.E. Ezebilo. 2014. "More or Less Moose: How Is the Hunting Value Affected?" *Scandinavian Journal of Forest Research* 29: 170–73.
- McCarthy, J., and G. Weetman. 2006. "Age and Size Structure of Gap-Dynamic, Old-Growth Boreal Forest Stands in Newfoundland." *Silva Fennica* 40: 209-30.
- McInnes, P.F., R.J. Naiman, J. Pastor, and Y. Cohen. 1992. "Effects of Moose Browsing on Vegetation and Litter of the Boreal Forest, Isle Royale, Michigan, USA." *Ecology* 73: 2059–75.
- McLaren, B. E., and R. O. Peterson. 1994. "Wolves, Moose, and Tree Rings on Isle Royale." *Science* 266 (5190): 1555–58.
- Piao, S., S. Sitch, P. Ciais, P. Friedlingstein, P. Peylin, X. Wang, A. Alsröm et al. 2013. "Evaluation of Terrestrial Carbon Cycle Models for their Response to Climate Variability and to CO<sub>2</sub> Trends." *Global Change Biology* 19: 2117–32.
- Randveer, T., and R. Heikkilä. 1996. "Damage Caused by Moose Alces Alces by Bark Stripping of *Picea Abies*." *Scandinavian Journal of Forest Research* 11 (1–4): 153–58.
- Schmitz, O. J. and S.J. Leroux, S. J. 2020. "Food Webs and Ecosystems: Linking Species Interactions to the Carbon Cycle." *Annual Review of Ecology, Evolution, and Systematics*, 51: 271–295.
- Schmitz, O.J., E. Post, C.E. Burns, and K.M. Johnston. 2003. "Ecosystem Responses to Global Climate Change: Moving Beyond Color-mapping." *BioScience* 53: 1199-1205.
- Schmitz, O.J., P.A. Raymond, J.A. Estes, W.A. Kurz, G.W. Holtgrieve, M.E. Ritchie, D.E. Schindler, et al. 2014. "Animating the Carbon Cycle." *Ecosystems* 7: 344-59.
- Schoener, T.W. 1973. "Population growth regulated by intraspecific competition for energy or time: Some simple representations." *Theoretical Population Biology* 4: 56-84.
- Solberg, Erling J, H. Sand, J Linnell, O Strand, and P Wabakken. 2003. "The Effects of Large Carnivores on Wild Ungulates in Norway: Implications for Ecological Processes, Harvest and Hunting." *NINA Fagrappport*, no. 63.
- Spalinger, D.E. and N.T. Hobbs. 1992. "Mechanisms of foraging in mammalian herbivores: new models of functional response." *American Naturalist* 140:325-48.



Tilman, D. 1982. *Resource Competition and Community Structure*. Princeton University Press, Princeton, NJ.

United Nations Environment Programme. 2009. *The Natural Fix? The Role of Ecosystems in Climate Mitigation: A UNEP Rapid Response Assessment*.  
<https://wedocs.unep.org/20.500.11822/7852>.

Wam, H.K., O. Hofstad, E. Nævdal, and P. Sankhayan. 2005. "A Bio-Economic Model for Optimal Harvest of Timber and Moose." *Forest Ecology and Management* 206: 207–19.

Watson, R.T., et al., 2000. *Land use, land-use change and forestry: a special report of the Intergovernmental Panel on Climate Change*. Cambridge University Press.

Zaehle, S., B.E. Medlyn, M.G. De Kauwe, A.P. Walker, M.C. Dietze, T. Hickler, T., Y. Luo et al. 2014. "Evaluation of 11 Terrestrial Carbon–nitrogen Cycle Models Against Observations from Two Temperate Free-Air CO<sub>2</sub> Enrichment Studies." *New Phytologist* 202: 803–22.